The Plant Cell, Vol. 31: 602–626, March 2019, www.plantcell.org © 2019 ASPB.

LARGE-SCALE BIOLOGY ARTICLE

Hierarchical Transcription Factor and Chromatin Binding Network for Wood Formation in *Populus trichocarpa*[OPEN]

Hao Chen,[a,b,c,1] Jack P. Wang,[a,b,1] Huizi Liu,[a] Huiyu Li,[a] Ying-Chung Jimmy Lin,[a,d,e] Rui Shi,[b] Chenmin Yang,[b] Jinghui Gao,[a] Chenguang Zhou,[a] Quanzi Li,[f] Ronald R. Sederoff,[b] Wei Li,[a,b,2] and Vincent L. Chiang[a,b,g,2]

[a] State Key Laboratory of Tree Genetics and Breeding, Northeast Forestry University, Harbin, 150040, China
[b] Forest Biotechnology Group, Department of Forestry and Environmental Resources, North Carolina State University, Raleigh, North Carolina 27695
[c] Department of Genetics, North Carolina State University, Raleigh, North Carolina 27695
[d] Department of Life Sciences, College of Life Science, National Taiwan University, Taipei, 10617, Taiwan
[e] Institute of Plant Biology, College of Life Science, National Taiwan University, Taipei 10617, Taiwan
[f] State Key Laboratory of Tree Genetics and Breeding, Chinese Academy of Forestry, Beijing 100091, China
[g] Department of Forest Biomaterials, North Carolina State University, Raleigh, North Carolina 27695

ORCID IDs: 0000-0002-6415-993X (H.C.); 0000-0002-5392-0076 (J.P.W.); 0000-0001-8853-2690 (H. Liu.); 0000-0002-7704-9721 (H. Li.); 0000-0001-7120-4690 (Y.-C.L.); 0000-0001-9070-1369 (R.S.); 0000-0001-5442-9783 (C.Y.); 0000-0002-8190-855X (J.G.); 0000-0001-6414-4693 (C.Z.); 0000-0002-7405-4402 (Q.L.); 0000-0001-6819-7047 (R.R.S.); 0000-0002-4407-9334 (W.L.); 0000-0002-7152-9601 (V.L.C.)

Wood remains the world's most abundant and renewable resource for timber and pulp and is an alternative to fossil fuels. Understanding the molecular regulation of wood formation can advance the engineering of wood for more efficient material and energy productions. We integrated a black cottonwood (*Populus trichocarpa*) wood-forming cell system with quantitative transcriptomics and chromatin binding assays to construct a transcriptional regulatory network (TRN) directed by a key transcription factor (TF), PtrSND1-B1 (secondary wall-associated NAC-domain protein). The network consists of four layers of TF–target gene interactions with quantitative regulatory effects, describing the specificity of how the regulation is transduced through these interactions to activate cell wall genes (effector genes) for wood formation. PtrSND1-B1 directs 57 TF–DNA interactions through 17 TFs transregulating 27 effector genes. Of the 57 interactions, 55 are novel. We tested 42 of these 57 interactions in 30 genotypes of transgenic *P. trichocarpa* and verified that ~90% of the tested interactions function in vivo. The TRN reveals common transregulatory targets for distinct TFs, leading to the discovery of nine TF protein complexes (dimers and trimers) implicated in regulating the biosynthesis of specific types of lignin. Our work suggests that wood formation may involve regulatory homeostasis determined by combinations of TF–DNA and TF–TF (protein–protein) regulations.

INTRODUCTION

Wood is formed in perennial angiosperms through the differentiation of the vascular cambium into xylem cells followed by secondary wall thickening due to the biosynthesis and deposition of three major components: cellulose, hemicellulose, and lignin (Evert, 2006). Wood is a composite of these three components where long cellulose microfibrils impart tensile strength, shorter hemicelluloses establish carbohydrate cross-linking, and lignin as a phenolic polymer fills in and cross-links the carbohydrate matrix (Albersheim et al., 2011). Similar to many processes of cellular development and differentiation, wood formation is controlled by transcriptional regulatory networks (TRNs; Lee et al., 2002; Levine and Davidson, 2005; Lin et al., 2013; Taylor-Teeples et al., 2015) consisting of multiple layers of transcription factor (TF)–target gene interactions (TF–DNA interactions; Müller, 2001; Hobert, 2008; Gerstein et al., 2010; modEncode Consortium et al., 2010; Niu et al., 2011; Lin et al., 2013). The elements of a TF–DNA TRN in wood formation are still in the early stages of identification.

A TF–target DNA interaction can be reliably identified in vivo by chromatin immunoprecipitation (ChIP; Solomon et al., 1988). However, ChIP does not reveal the transregulation effects on the target gene. A combined analysis of ChIP and the induced transcript level of the TF's direct target will provide quantitative information about the regulatory specificity (direct activation or suppression) and strength. The combination of ChIP sequencing and RNA sequencing (RNA-seq) has been used to discover functional TRNs in animal and plant development, using cell cultures or transgenics at different developmental stages where specific sets of TFs are induced (Gerstein et al., 2010; Roy and The

[1] These authors contributed equally to this work.
[2] Address correspondence to weili2015@nefu.edu.cn and vchiang@ncsu.edu. The author responsible for distribution of materials integral to the findings presented in this article in accordance with the policy described in the Instructions for Authors (www.plantcell.org) is: Vincent L. Chiang (vchiang@ncsu.edu).
[OPEN]Articles can be viewed without a subscription.
www.plantcell.org/cgi/doi/10.1105/tpc.18.00620

IN A NUTSHELL

Background: Wood develops in trees as a biological composite of three cell-wall components, cellulose (a fibrous polysaccharide), hemicellulose (amorphous polysaccharides) and lignin (a phenolic polymer). Wood has long been used for timber, paper and energy production. The production efficiency can be drastically improved using genetically tailored wood. To do that, we need to understand the genetic regulation of wood formation. Knowledge of genes underlying the biosynthesis of the three wood components is extensive. However, little is known about the regulatory system, i.e., the identity and network arrangement/hierarchy of the key regulators called transcription factors (TFs), that coordinates the expression of combinations of component genes for wood formation. We wanted to construct such a transcriptional regulatory network (TRN) using a model tree species, *Populus trichocarpa* (black cottonwood).

Question: A TRN typically consists of 3 to 5 hierarchical layers of TF-DNA interactions. We focused on a high-level wood formation TF, PtrSND1-B1. We wanted to know how a TRN transduces the regulation of PtrSND1-B1 to activate the component genes for wood formation.

Findings: Using a transient *P. trichocarpa* wood-cell system and 30 transgenic *P. trichocarpa* lines, we revealed that PtrSND1-B1 mediates a four-layered TRN, directing 57 specific TF–DNA interactions through 17 TFs to regulate 27 cell-wall component genes for wood formation. We generated quantitative information about regulatory specificity (direct activation or suppression) and strength of these 57 interactions in the PtrSND1-B1 TRN. The TRN also revealed common targets for distinct TFs, leading to the discovery of 9 novel TF–protein complexes implicated in wood formation. We also deduced a genome-wide AtSND-1 TRN for the model plant *Arabidopsis thaliana*. The AtSND-1 TRN has 50 specific TF–DNA interactions. Only 7 of these 50 interactions were found in the PtrSND1-B1 wood formation TRN, indicating wood formation is not a function in herbaceous plants.

Next steps: Genetic regulation of wood formation is best studied in woody species because of their abundance and specialization in secondary xylem. The complete hierarchical TRN should be investigated further to reveal how all cell wall genes are regulated to affect wood phenotypes.

modEncode Consortium et al., 2010; Cheng et al., 2011; Niu et al., 2011; Lin et al., 2013; Song et al., 2016). The TF-directed functional TRNs are arranged in well-structured hierarchies (Davidson et al., 2002; Yu and Gerstein, 2006; Erwin and Davidson, 2009; Bhardwaj et al., 2010; Davidson, 2010; Lin et al., 2013).

In a TF TRN, high-level TFs act as master switches or key receptors to activate the network and initiate a coordinated process and control mid-level TFs that, in turn, regulate effector genes (e.g., cell wall component genes) at the bottom of the network that are directly responsible for implementing specific processes (e.g., wood formation; Yu and Gerstein, 2006; Bhardwaj et al., 2010; Yan et al., 2010; Lin et al., 2013; Song et al., 2016; Yang et al., 2017). Typically, three to five hierarchical layers may be involved in TRNs for growth and development in animals (Gerstein et al., 2010; Roy and The modEncode Consortium et al., 2010; Cheng et al., 2011; Niu et al., 2011) or in plants (Lin et al., 2013; Lu et al., 2013; Taylor-Teeples et al., 2015; Song et al., 2016; Yang et al., 2017).

In addition to the combined ChIP sequencing and RNA-seq approach, a hierarchical TF TRN may also be established using a yeast one-hybrid (Y1H) screening method. Y1H can identify a TF that interacts with specific *cis*-acting elements in the promoter of a target gene (Li and Herskowitz, 1993; Wang and Reed, 1993). Therefore, starting from the promoter of the effector genes (as the bottom layer of a TRN), the Y1H method can screen for TFs that directly interact with the effector genes. The promoter of these TFs may then be used to screen for their *trans*-acting TFs and then to proceed stepwise (a bottom-up approach) to reveal a hierarchical TRN for the process. The Y1H-based approach has been applied to construct many complex growth and development TRNs in humans (Reece-Hoyes et al., 2011), nematodes (*Nematoda*; Deplancke et al., 2004, 2006; Vermeirssen et al., 2007), and fruit flies (*Drosophila melanogaster*; Hens et al., 2011). In Arabidopsis (*Arabidopsis thaliana*), Y1H was used to screen 45 effector genes of root xylem cell wall formation for interactions with 467 candidate TFs. A five-layer TRN was constructed that included 209 TFs regulating 617 TF–DNA interactions, representing the most comprehensive cell wall TRN to date in Arabidopsis (Taylor-Teeples et al., 2015). The Y1H system is useful for the identification of interactions in vitro. The resulting interactions require in vivo validation, such as using ChIP, to demonstrate their biological and functional relevance.

Other studies of xylem cell wall biosynthesis in Arabidopsis using mutation and coexpression analyses have led to a regulation model that consists of four gene groups: (1) first-layer master switches (NAC genes; NAM, ATAF1/2, and CUC2 genes), (2) second-layer master switches (MYB [myeloblastosis] genes; v-myb avian myeloblastosis viral oncogene homologs), and (3) downstream regulators (TF genes) regulating (4) genes for secondary cell walls (McCarthy et al., 2009; Zhong et al., 2010a; Ko et al., 2012, 2014; Wang and Dixon, 2012; Zhong and Ye, 2012; Nakano et al., 2015). These studies are lacking in detail on the transregulatory specificity and hierarchical structure, which are essential in a TRN (Lee et al., 2002; Levine and Davidson, 2005; Hobert, 2008; Gerstein et al., 2010; Roy and The modEncode Consortium et al., 2010; Niu et al., 2011; Lin et al., 2013).

Many TFs have been studied in tree species for their potential role in regulating cell wall component genes in wood formation. In *Populus*, these TFs include PtrMYB2/3/20/21, PttMYB021a, PtrWNDs (wood-associated NAC domain proteins), PtoMYB92, PtrMYB152, PtoMYB0216, PtrSND1-A2^{IR}, and PtrWRKY19 (conserved WRKYGQK domain protein), while EgMYB1 and EgMYB2 have been studied in *Eucalyptus*; PtMYB1, PtMYB4, and PtMYB8 in *Pinus*; and PgMYB1/8 and PgMYB14/15 in *Picea* (Patzlaff et al., 2003a, 2003b; Karpinska et al., 2004; Goicoechea

et al., 2005; Legay et al., 2010; Zhong et al., 2010a, 2010b; Ohtani et al., 2011; Li et al., 2012, 2015; Tian et al., 2013; Wang et al., 2014b; Yang et al., 2016). These studies have provided information on the regulatory effects of TFs but little information on the regulatory specificity and quantitative interactions. Some of these effects were inferred from heterologous transgenic systems (stable or transient), which are inadequate for a rigorous analysis of hierarchical transcriptional regulation.

To learn more about the transcriptional specificity of wood formation, we have focused on a specific wood-forming tissue (stem-differentiating xylem [SDX]) in a single woody species, black cottonwood (*Populus trichocarpa*) clone Nisqually-1, to study the direct TF–target gene interactions for the construction of a wood formation TRN. We have focused on this P. trichocarpa clone because it has a well-annotated genome sequence and TF families have been identified (Jin et al., 2017). Because many TFs require a tissue-specific partner for regulation of the target DNA (Farnham, 2009; Moreno-Risueno et al., 2010; Faraco et al., 2011), specific cells or tissues expressing the process of interest should be used for meaningful interpretations of TF–DNA interactions. For example, leaf mesophylls (Zhong et al., 2006, 2010a, 2011; Xie et al., 2018) are not an appropriate system for studying xylem cell wall or wood formation.

In previous work, we constructed a two-layer PtrSND1-B1 (secondary wall-associated NAC-domain protein, a NAC TF) TRN associated with wood formation in *P. trichocarpa* (Lin et al., 2013). Here, we present a top-down approach, one layer of TF–DNA interaction at a time, for the discovery of a more extensive PtrSND1-B1–controlled multilayer TRN for wood formation. To do this, we developed a wood formation cell system from protoplasts of *P. trichocarpa* SDX (Li et al., 2012; Lin et al., 2013, 2017). We integrated this system with analyses of RNA-seq, TF-epitope ChIP transregulation, yeast two-hybrid (Y2H), bimolecular fluorescence complementation (BiFC), and transgenic expression in *P. trichocarpa*. The integrated system established a PtrSND1-B1–directed TF–DNA and TF–TF (protein–protein) hierarchical regulatory network that regulated the expression of 27 cell wall genes. All TF–DNA interactions in this network were validated and quantified. We also analyzed the functions of ~476 TFs (Supplemental Data Set 1) from 31 plant species to define TRNs for identifying functional conservation among these TRNs. Our approach for TRN discovery can be exploited to understand other complex biological processes in plants.

RESULTS

PtrMYB021 and PtrMYB074 Are Transcriptional Activators in Fiber and Vessel Cells of SDX in *P. trichocarpa*

In our previously established PtrSND1-B1–directed TRN, PtrSND1-B1, the top-layer TF, directly regulates 76 genes, including 66 enzyme-coding genes and 10 TF genes on the second layer (Lin et al., 2013). These 66 enzyme genes do not include any of the known key cell wall component genes (Shi et al., 2017), suggesting that these wood formation genes are regulated by the second-layer or lower layer TFs in a TRN. Among the 10 second-layer TFs, PtrMYB021 (*Potri.009G053900*) and PtrMYB074 (*Potri.015G082700*, also named PtrMYB050; Lin et al., 2013) are the likely wood formation regulators because they are most highly and specifically expressed in SDX (Supplemental Figure 1). Therefore, we started from PtrMYB021 and PtrMYB074 to continue the construction of the PtrSND1-B1–based wood formation TRN.

To begin, we determined whether *PtrMYB021*, *PtrMYB074*, and their upstream regulator *PtrSND1-B1* are coexpressed within wood-forming cells, using laser capture microdissection (LCM) coupled with reverse transcription quantitative PCR (RT-qPCR; Figure 1). Differentiating fiber and vessel cells, the two major wood-forming cell types, were isolated by LCM from stem cross sections of *P. trichocarpa* (Figures 1A to 1D) for transcript quantification. RT-qPCR showed that these three TFs are coexpressed in both fiber and vessel cells (Figures 1E to 1G).

We next analyzed the subcellular localizations of PtrMYB021 and PtrMYB074 proteins in wood-forming cells. PtrSND1-B1 was demonstrated to be a nuclear protein in wood-forming cells (Lin et al., 2013). *P. trichocarpa* SDX protoplasts were transfected with *35S-PtrMYB021-sGFP* (green fluorescent protein) and *35S-H2A-mCherry*, a nuclear marker, or *35S-PtrMYB074-sGFP* and the same nuclear marker. The green fluorescence signals of GFPfused PtrMYBs were colocalized in the nucleus along with the red fluorescence signals of H2A-mCherry (Figures 1H to 1M), demonstrating that PtrMYB021 and PtrMYB074 are also nuclear proteins involved in wood formation (Figures 1N to 1P). We then investigated the regulatory roles of PtrMYB021 and PtrMYB074 in SND1-B1–mediated TRN. To do this, we designed a top-down approach integrating the SDX protoplast system (Lin et al., 2013) with quantitative transcriptomic (RNA-seq and RT-qPCR) and chromatin binding (ChIP-PCR) analyses (Figure 2).

Workflow for Constructing the Hierarchical TRN

Six key steps were used for TRN construction and validation (Figure 2). In step 1 (overexpression in SDX protoplasts), *PtrMYB021* and *PtrMYB074* were overexpressed individually in the *P. trichocarpa* SDX protoplasts that were then analyzed by RNA-seq to identify differentially expressed genes (DEGs). In step 2 (DEG specificity), the DEGs were screened for xylem cell wall biosynthetic and TF genes. In step 3 (ChIP), the promoters of these cell wall and TF genes were characterized by ChIP to identify those directly bound by PtrMYB021 and PtrMYB074. These direct cell wall and TF target genes of PtrMYB021 and PtrMYB074 form the third layer of the TRN. In step 4 (overexpression in SDX protoplasts), the third-layer TFs were each overexpressed in the SDX protoplasts, and the responses were quantified by RT-qPCR to determine the transcript levels of 36 cell wall component genes to identify those TFs that affect the expression of these cell wall genes. In step 5 (screening for direct effects), the TF genes affecting cell wall gene expression were assayed by ChIP to screen for direct regulation of cell wall genes. These TFs and cell wall genes constitute the third and the bottom layer, respectively, of the PtrSND1-B1–directed wood formation TRN. And in step 6 (in vivo validation), key regulatory effects of the TRN were validated in transgenic *P. trichocarpa*.

Genome-Wide PtrMYB021 and PtrMYB074 Regulation of Wood Xylem Formation

SDX protoplasts were transfected with *pUC19-35S-PtrMYB021-35S-sGFP* or *pUC19-35S-Ptr-MYB074-35S-sGFP*, held for 7 h,

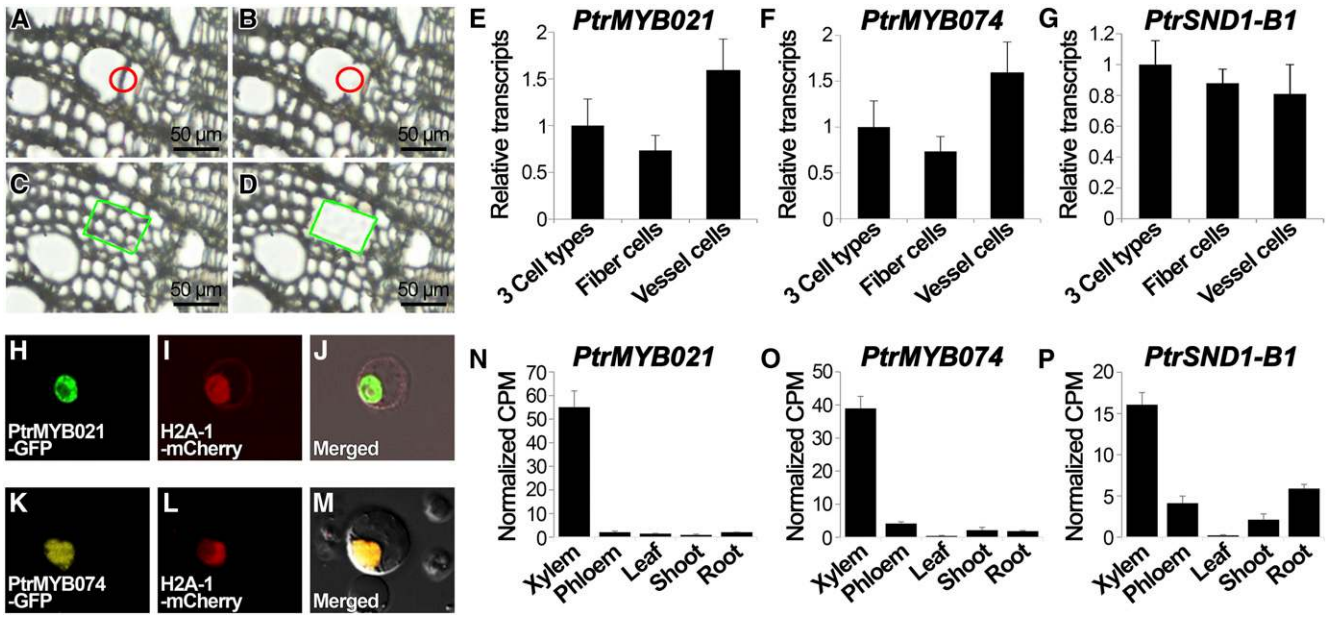

Figure 1. Xylem Fiber and Vessel Cell–Specific Expression, Subcellular Localization, and Transcriptional Activity of PtrMYB021 and PtrMYB074.

(A) to **(D)** Xylem cross section before **(A)** and after **(B)** LCM isolation of vessel cells. Xylem cross section before **(C)** and after **(D)** LCM isolation of fiber cells. Red circles in **(A)** and **(B)** indicate the dissected vessel cells, and green rectangles in **(C)** and **(D)** indicate the dissected fiber cells. Scale bar = 50 μm in **(A)** to **(D)**.

(E) to **(G)** Quantitative measurement of transcript abundances of *PtrSND1-B1* **(E)**, *PtrMYB021* **(F)**, and *PtrMYB074* **(G)** in SDX cells isolated by LCM. The label 3 Cell types denote fiber, vessel, and ray cells, the three major cell types in SDX. Relative transcript abundance and SE are calculated from three biological replicates.

(H) to **(M)** Subcellular location of GFP fused PtrMYB021 (H-J) and PtrMYB074 proteins (in **[K]** to **[M]**). The MYB021-GFP signal **(H)**, the MYB074-GFP signal **(K)**, and the H2A-mCherry signals **(I)** and **(L)**, and merged images **(J)** and **(M)** are shown.

(N) to **(P)** Transcript abundance (normalized count per million [CPM] reads) of *PtrMYB021* **(N)**, *PtrMYB074* **(O)**, and *PtrSND1-B1* **(P)** in five *P. trichocarpa* tissues: xylem, phloem, leaf, shoot, and root. Error bars represent 1 SE of three biological replicates.

and analyzed by RNA-seq (Figure 2, step 1; see Methods). Protoplasts transfected with *pUC19-35S-sGFP* plasmids were used as the control. Three independent experiments were performed for TF-transfected and control SDX protoplasts. The transcriptomes of the PtrMYB021- or PtrMYB074-transfected protoplasts were compared with the control (sGFP) transcriptomes to identify DEGs. Overexpression of PtrMYB021 affected the expression of 164 genes (DEGs; fold change > 2 or < 0.8, false discovery rate [FDR] < 0.05) and PtrMYB074 affected 135 genes (fold change > 2 or < 0.8, FDR < 0.05; Supplemental Figure 2; Supplemental Data Sets 2 and 3). The expression of these affected genes was all upregulated, demonstrating the transactivation function of PtrMYB021 and PtrMYB074 in vivo. We then focused on the TF and the cell wall biosynthetic genes in the 164 DEGs activated by PtrMYB021 and the 135 genes activated by PtrMYB074 to continue the TRN construction.

Based on the annotation of the *P. trichocarpa* genome (Phytozome 11; https://phytozome.jgi.doe.gov/pz/portal.html) and the plant TF database (Goodstein et al., 2012; Jin et al., 2017), we identified 17 TFs (DEG1 to DEG17 in Supplemental Data Set 2) from the 164 genes regulated by PtrMYB021 and 13 TFs (DEG1 to DEG13 in Supplemental Data Set 3) from the 135 genes regulated by PtrMYB074 (Figure 2, step 2). Gene ontology (GO) analysis (g:Profiler; http://biit.cs.ut.ee/gprofiler/) (Reimand et al., 2016) of the remaining genes identified those associated with cell wall biosynthesis. Most of the significant GO biological process terms for the PtrMYB021- and PtrMYB074-regulated DEGs belong to cell wall biosynthetic processes, including the plant-type secondary cell wall biogenesis, lignin metabolic process, and lignin catabolic process (Supplemental Tables 1 and 2). We found that 19 PtrMYB021-regulated genes (Supplemental Table 3) and 18 PtrMYB074-regulated genes (Supplemental Table 4) are associated with these cell wall biosynthetic processes. These genes include those encoding laccases and peroxidases for lignin polymerization, *phenylalanine ammonia-lyase 2* (*PAL2*) for monolignol biosynthesis, *fragile fiber 1* (*FRA1*) and *irregular xylem 6* (*IRX6*) for cellulose biosynthesis, and *IRX9* and *IRX14* for hemicellulose biosynthesis (Supplemental Tables 3 and 4).

Our *P. trichocarpa* tissue-specific RNA-seq data (GSE81077; Shi et al., 2017) revealed that 14 of the 19 cell wall biosynthetic process genes regulated by PtrMYB021 (highlighted in Supplemental Table 3) are expressed specifically and abundantly in SDX, compared with leaves, juvenile shoots, and stem-differentiating phloem (Supplemental Data Set 4A). Of the 18 cell wall biosynthetic process genes regulated by PtrMYB074, 13 (highlighted in Supplemental Table 4) are SDX abundant and specific (Supplemental Data Set 4B). We also examined the

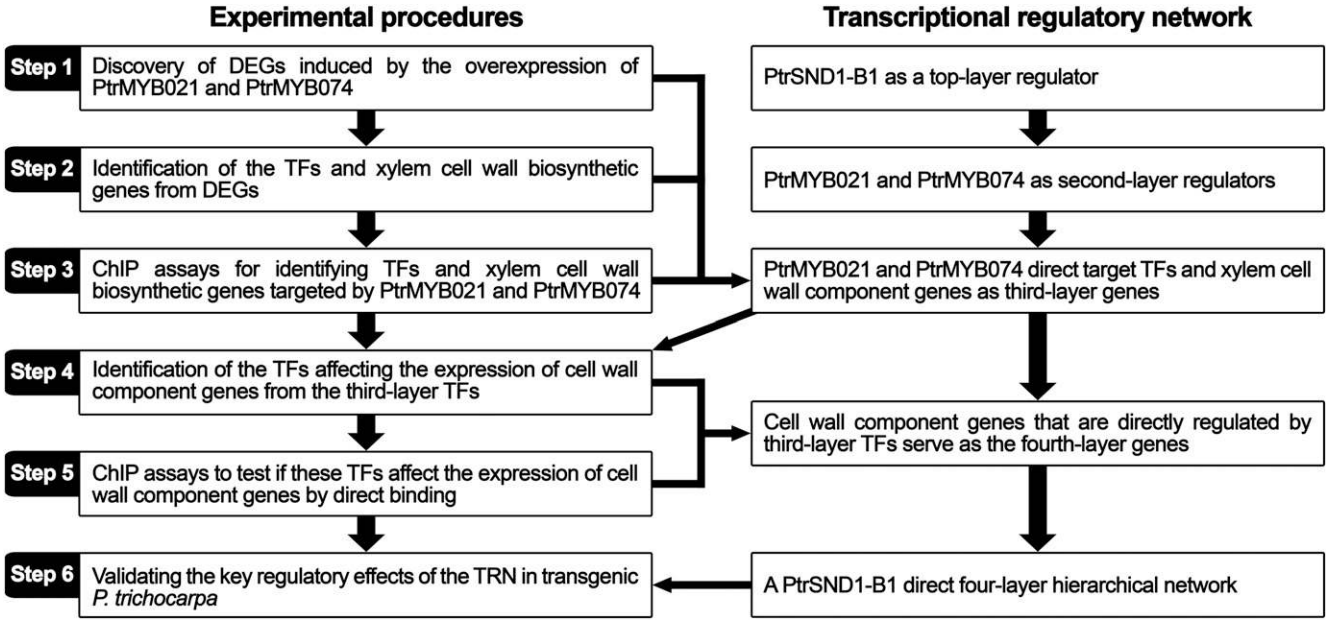

Figure 2. Methodology Flowchart.

Flowchart depicts a pipeline of how the PtrSND1-B1 four-layered network was constructed and validated using experimental approaches. The six-step experimental procedures were used for generating and validating the regulatory relationships between TFs and their target genes. These relationships were used for generating the TRN in wood formation.

tissue-specific expression of the TFs regulated by PtrMYB021 and PtrMYB074 and found that all these TFs are expressed in differentiating xylem (Supplemental Data Sets 5A and 5B).

In summary, PtrMYB021 overexpression activated the expression of 14 wood cell wall biosynthetic genes and 17 TFs, and PtrMYB074 overexpression upregulated 13 wood cell wall biosynthetic genes and 13 TFs (Supplemental Data Sets 2 and 3; Supplemental Tables 3 and 4; Figure 2, step 2). Of these 57 (14 + 17 + 13 + 13) TF target regulations, PtrMYB021-mediated activation of *PtrFRA1* (also known as *PtrGT47c*; Zhong et al., 2013) is the only one that has been previously demonstrated, based on promoter-GUS transactivation assays in Arabidopsis leaf protoplasts (Zhong et al., 2013). These 57 regulations are the outcome of the overall regulatory response and may or may not be the result of direct transregulation. We then used ChIP to determine which of these regulatory responses are induced by direct transregulation of PtrMYB021 and PtrMYB074 to discover the third layer of the TRN (Figure 2, step 3) and the TRN's regulatory specificity.

PtrMYB021-GFP and PtrMYB074-GFP Fusion Proteins Retain the Native Transregulation Activity and Were Used to Construct the ChIP-Based TRN

We overexpressed PtrMYB021-GFP and PtrMYB074-GFP fusion proteins individually in *P. trichocarpa* SDX protoplasts and performed ChIP on the transformed protoplasts using anti-GFP antibodies. We first tested whether the GFP-tagged MYBs retain their native transactivation function. To do this, PtrMYB021-GFP (*pUC19-35S-PtrMYB021-sGFP*) and the untagged PtrMYB021 (*pUC19-35S-Ptr-MYB021-35S-sGFP*) were independently overexpressed in SDX protoplasts. Protoplasts were also transfected with *pUC19-35S-sGFP* plasmids as the control. The transcript abundances of three genes (*Potri.005G129500*, *Potri.014G073700*, and *Potri.008G160000*) randomly selected from the 164 genes upregulated by PtrMYB021 were quantified by RT-qPCR. Both PtrMYB021-GFP and PtrMYB021 proteins can similarly upregulate the expression of the three randomly selected target genes (Supplemental Figure 3A). Likewise, PtrMYB074-GFP and PtrMYB074 could both upregulate three randomly selected PtrMYB074 target genes (*Potri.T138100*, *Potri.011G150300*, and *Potri.019G121700*) (Supplemental Figure 3B). Therefore, GFP fusions of PtrMYB021 and PtrMYB074 should be effective for identifying the direct targets of these PtrMYBs to establish the third layer of the TRN.

PtrMYB021 and PtrMYB074 Directly Regulate 12 Candidate Cell Wall Formation–Related Genes Forming the Third Layer of a Wood Formation TRN

We performed ChIP on the MYB-GFP–transformed protoplasts using anti-GFP antibodies. PCR amplification of the chromatin DNA products was performed for four fragments (fragments I to IV; Figure 3A; Supplemental Figure 4) of the ~2-kb promoter sequences upstream of each of the 14 cell wall biosynthetic genes (gray highlighting in Supplemental Table 3) regulated by PtrMYB021. Robust enrichment of PtrMYB021-GFP was observed in at least one of the four fragments in the 2-kb promoter of 8 of the 14 cell wall biosynthetic genes (Figure 3B). Therefore, the PtrMYB021 overexpression-mediated activation of 8 of these 14

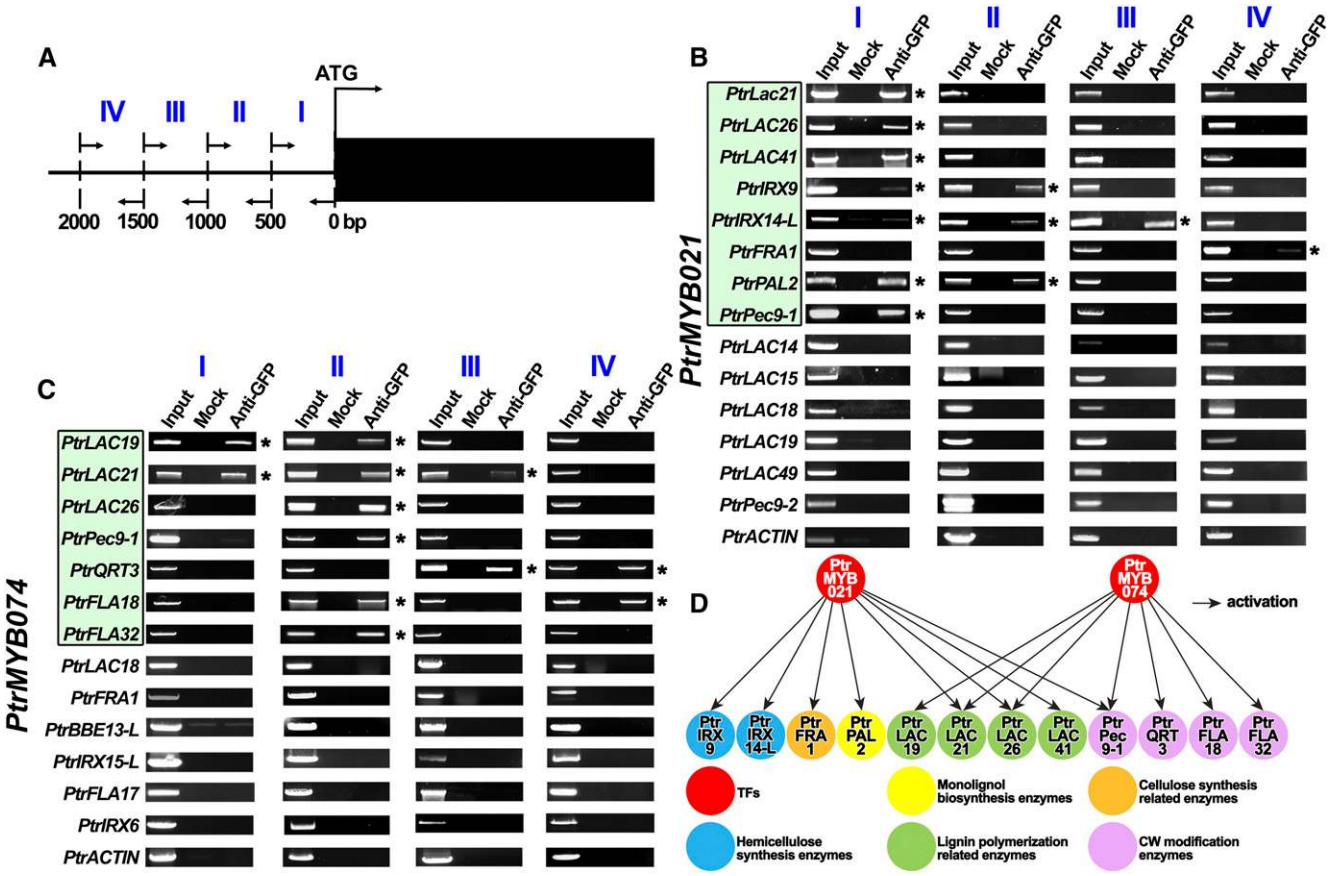

Figure 3. Identification of Cell Wall Biosynthetic Genes Directly Targeted by PtrMYB021 and PtrMYB074 by ChIP Assays.

(A) Approximate location of the promoter fragments (I to IV) amplified by PCR following ChIP assays. Rectangle shows the gene, and the line represents a gene promoter. The arrowheads show the approximate location of the promoter region that was assigned for designing primers for PCR amplification. The precise locations of the promoter sequences tested in ChIP-PCR are shown in Supplemental Figure 4.

(B) and **(C)** ChIP-PCR assays of cell wall biosynthetic genes regulated by PtrMYB021 **(B)** and PtrMYB074 **(C)**. Four promoter fragments of each target gene were amplified by PCR following ChIP assays. Input, mock, and anti-GFP represent PCR reactions using the chromatin preparations before immunoprecipitation, immunoprecipitated with preimmune serum and immunoprecipitated with anti-GFP antibody, respectively. Four independent biological replicates for each ChIP assay were performed, and the results of one biological replicate are presented. A TF–DNA interaction is considered true when at least three of the four biological replicates are positive. The direct targets of PtrMYB021 and PtrMYB074 are framed in **(B)** and **(C)**, and the indirect targets are not. The promoter fragments that can be bound by PtrMYB021 or PtrMYB074 proteins are marked with an asterisk (*). The promoter fragments of *PtrACTIN* were assayed as a negative control.

(D) Diagram depicting the regulation of PtrMYB021 and PtrMYB074 for the cell wall (CW) biosynthetic genes. Arrows indicate the protein–DNA regulatory interaction with activation ability.

genes (Supplemental Table 3) was likely the result of direct transregulation by PtrMYB021. These eight PtrMYB021 direct targets include genes involved in lignin polymerization (*PtrLAC21*, *PtrLAC26*, and *PtrLAC41*; Ranocha et al., 2002; Berthet et al., 2011; Lu et al., 2013), hemicellulose biosynthesis (*PtrIRX9* and Ptr*IRX14-L*; Wu et al., 2010; Lee et al., 2014), cellulose biosynthesis (*PtrFRA1*; Zhu et al., 2015), monolignol biosynthesis (*PtrPAL2*; Wang et al., 2014a), and cell wall modification (*PtrPec9-1*; de Souza et al., 2014).

Similarly, ChIP-PCR (Figure 3C) and RNA-seq (Supplemental Data Set 3) analyses demonstrated that of the 13 PtrMYB074-activated cell wall biosynthetic genes (gray highlighting in Supplemental Table 4), seven are the likely direct targets. These targets include lignin polymerization genes (*PtrLAC19*, *PtrLAC21*, and *PtrLAC26*; Lu et al., 2013) and cell wall modification genes (*PtrPec9-1*, *PtrFLA18*, *PtrFLA32*, and *PtrQRT3*; Figure 3C; Rhee et al., 2003; MacMillan et al., 2010; de Souza et al., 2014). PtrMYB074 binds to at least one unique site in the 2-kb promoter of these seven direct targets (Figure 3C).

In summary, it is highly likely that PtrMYB021 and PtrMYB074 directly activate eight and seven cell wall formation genes, respectively. Of these 15 targets, 12 are uniquely regulated by the two MYBs and three are redundantly controlled by both MYBs, indicating these MYBs' diverse regulatory functions in controlling wood formation. The three redundant targets are *PtrLAC21*, *PtrLAC26*, and *PtrPec9-1* (Figure 3D).

PtrMYB021 and PtrMYB074 Also Directly Regulate 15 Unique TF Genes as the Third-Layer Constituents of the TRN

We next used the same GFP fusion and anti-GFP antibody–based ChIP approach together with RNA-seq to identify the candidate TF gene targets of these two PtrMYBs (Figure 2, step 3). Four chromatin fragments in the ~2-kb promoter of each tested TF gene were PCR amplified for ChIP analysis (Figure 4A; Supplemental Figure 5). We found that promoters of 10 of the 17 PtrMYB021-activated TF genes (Supplemental Data Set 6) were bound by PtrMYB021-GFP at one or more of the four fragments (Figure 4B). These 10 TF genes likely direct TF targets of PtrMYB021 and include four MYBs, three Bel-like homeodomains (wood Bel-like TFs [WBLHs]), two NACs, and one GRAS (GAI, RGA, SCR; Supplemental Data Set 6). PtrMYB074-GFP binds to the promoters of 10 of the 13 PtrMYB074-activated TF genes at a single or multiple sites (Figure 4C). The 10 direct targets of PtrMYB074 included six MYBs, three NACs, and one WBLHTF (Figure 4C; Supplemental Data Set 6). Together, PtrMYB021 and PtrMYB074 directly regulate 15 unique TFs, with five being common regulatory targets—*PtrMYB059*, *PtrMYB090*, *PtrMYB161*, *PtrNAC123*, and *PtrWBLH2* (Figure 4D)—demonstrating possible specific cooperative or combinatorial roles of PtrMYB021 and PtrMYB074 in transcriptional regulation. Two, PtrMYB090 and PtrNAC123 (also known as PtrSND2/3-A1; Li et al., 2012), of the 15 TFs have previously been suggested to be associated with secondary cell wall formation (Chai et al., 2014) and cell wall crystallinity (Porth et al., 2013). The specific transregulatory effects of these 15 TFs on wood cell wall formation are unknown. We therefore investigated the regulatory roles (Figure 2, step 4) of

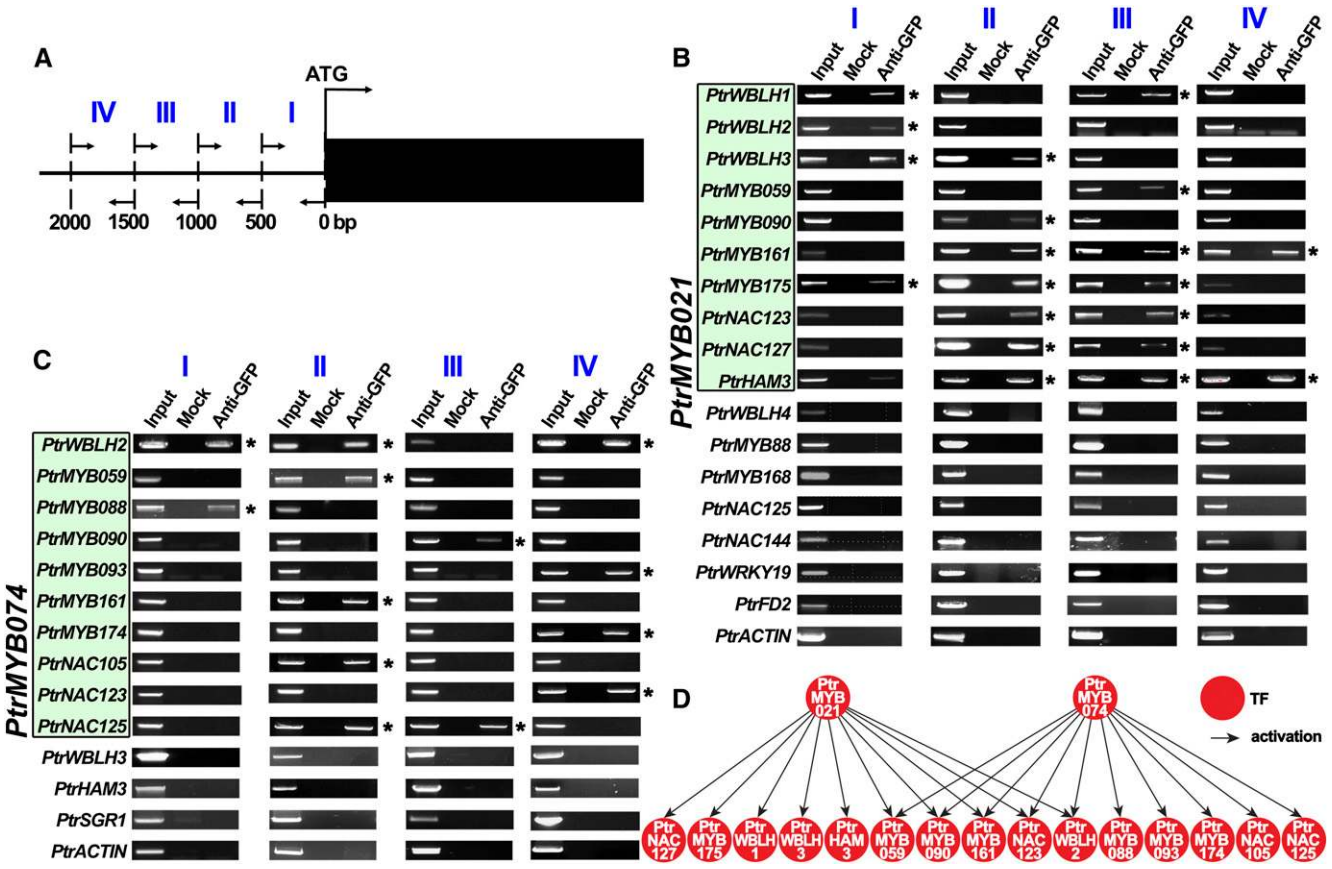

Figure 4. ChIP Identification of TF Genes Directly Targeted by PtrMYB021 and PtrMYB074.

(A) Approximate locations of the promoter sequences amplified by PCR following the ChIP assays, as described in Figure 3. The precise locations of the promoter sequences tested in ChIP-PCR are shown in Supplemental Figure 5.

(B) and **(C)** ChIP-PCR assays of TF genes from PtrMYB021-regulated genes **(B)** and PtrMYB074-regulated genes **(C)**. Four promoter fragments of each target gene were amplified by PCR following ChIP assays. Input, mock, and anti-GFP represent PCR reactions using the chromatin preparations before immunoprecipitation, immunoprecipitated with preimmune serum, and immunoprecipitated with anti-GFP antibody, respectively. Four independent biological replicates for each ChIP assay were performed, and the results of one biological replicate are presented. A TF–DNA interaction is considered true when at least three of the four biological replicates are positive. The direct targets of PtrMYB021 and PtrMYB074 are framed in **(B)** and **(C)**, and the indirect targets are not. The promoter fragments that can be bound by PtrMYB021 or PtrMYB074 proteins are marked with an asterisk (*). For these experiments, the promoter fragments of *PtrACTIN* were assayed as a negative control.

(D) Diagram showing that PtrMYB021 and PtrMYB074 directly regulate the TF genes. The arrows indicate the protein–DNA regulatory interaction with activation ability.

these 15 direct TF targets of PtrMYB021 and PtrMYB074 on the expression of the wood cell wall component genes using our SDX protoplast system.

PtrMYB021 and PtrMYB074 Directly Regulate Nine TFs That Can Affect the Expression of a Majority of the Cell Wall Component Genes

Lignin, cellulose, and hemicellulose are the major components of the wood cell wall (Hägglund, 1952). Here, we focused on the direct regulation of PtrMYB021 and PtrMYB074 on monolignol and cellulose biosynthetic genes because genes involved in hemicellulose biosynthesis in tree species have not been clearly defined. We identified 36 cell wall component genes (Supplemental Data Set 7), including nine primary cell wall cellulose synthase genes (*PtrPRC1-2* and *PtrPRC1-3*; *PtrIXR1-1*, *PtrIXR1-2*, *PtrIXR1-3*, and *PtrIXR1-4*; *PtrRSW1-1* and *PtrRSW1-2*; and *PtrCesA9-3*; Suzuki et al., 2006; Kumar et al., 2009), five secondary cell wall cellulose synthase genes (*PtrCesA4*, *PtrCesA7*, *PtrCesA8*, *PtrCesA17*, and *PtrCesA18*; Suzuki et al., 2006; Kumar et al., 2009; Song et al., 2010), and 22 core monolignol biosynthetic genes from 11 families (*PAL*, *C4H*, *4CL*, *C3H*, *HCT*, *CSE*, *CCoAOMT*, *COMT*, *CAld5H*, *CCR*, and *CAD*; Shi et al., 2010b; Wang et al., 2014a, 2018).

We overexpressed in SDX protoplasts each of the 15 TFs that are directly regulated by PtrMYB021 and PtrMYB074, following the procedures described above for the overexpression of *PtrMYB021* and *PtrMYB074*. We used RT-qPCR to quantify transcript levels of the 36 cell wall genes in transfected SDX protoplasts overexpressing each TF and compared their expression to controls overexpressing sGFP alone, to identify DEGs. DEGs with a fold change > 2 (activation effect, $P < 0.1$) or < 0.8 (repression effect, $P < 0.1$) were considered regulated genes (Supplemental Data Set 8). Of the 36 cell wall component genes, 25 (Figure 5, green highlighting) were regulated by nine (Figure 5, yellow highlighting) of the 15 TFs. The 25 cell wall genes include all five secondary cell wall cellulose synthase genes, five of nine primary cell wall cellulose synthase genes, and 15 monolignol genes that represent nine of the 11 monolignol gene families. Therefore, these nine TFs are key regulators for cell wall

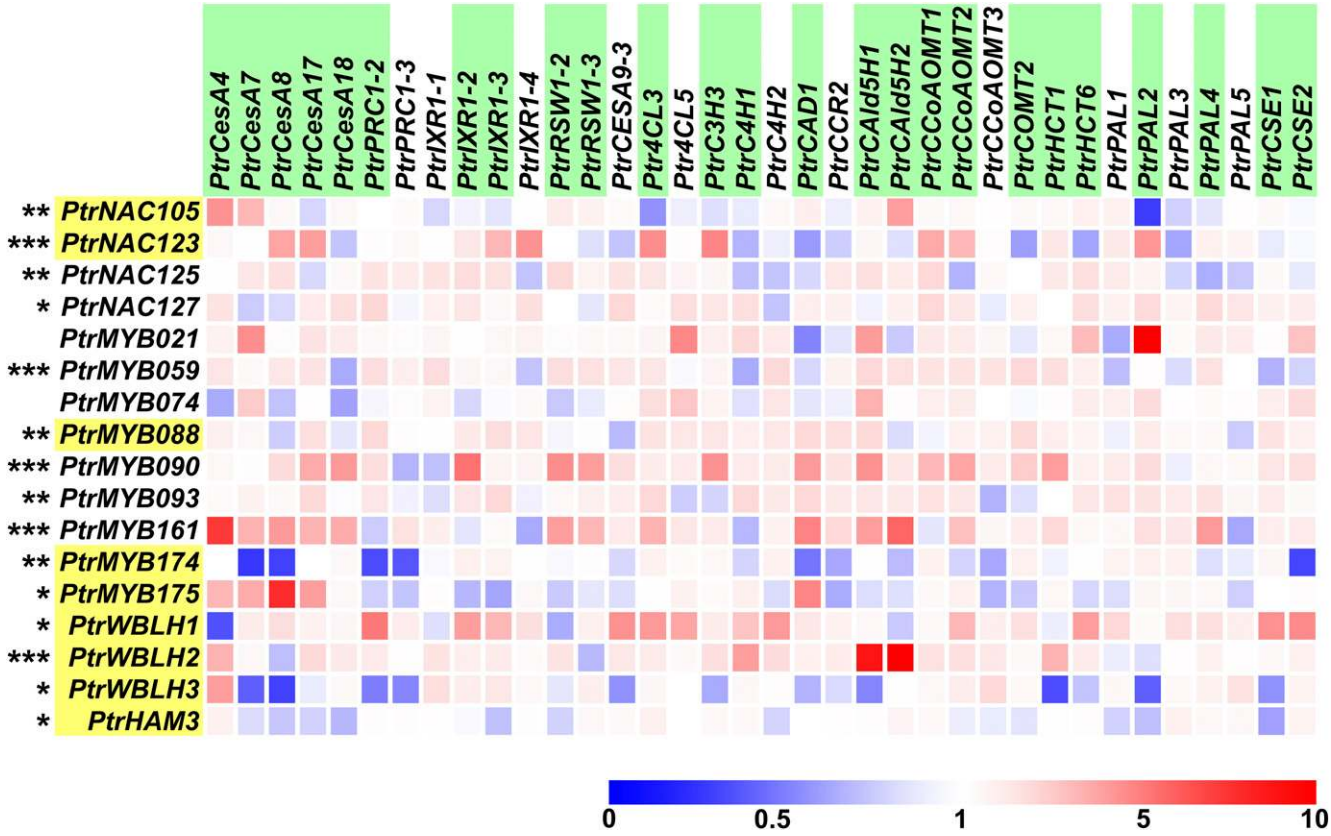

Figure 5. Expression Profiles of 36 Cell Wall Biosynthetic Genes in SDX Protoplasts Overexpressing Each of 15 TFs Directly Regulated by PtrMYB021 and PtrMYB074.

Heatmap represents the relative expression (fold change) of the genes in SDX protoplasts overexpressing each TF compared with the control. The average expression of three biological replicates is presented. Fold change and SE for RT-qPCR are shown in Supplemental Data Set 8. The overexpressed TFs are shown on left side, and the cell wall biosynthetic genes are shown in upper panel. Twenty-five (highlighted in green) of the 36 cell wall genes were regulated by nine TFs (highlighted in yellow). Color bar at the bottom depicts the relative expression levels, where blue, white, and red represent downregulation, no change, and upregulation, respectively. Asterisks represent genes regulated by PtrMYB021 (*), PtrMYB074 (**), or both PtrMYB021 and PtrMYB074 (***).

biosynthesis and wood formation. The results further demonstrated that a single TF can regulate (activate and repress, red and blue shades in Figure 5, respectively) multiple cell wall component genes and that many TFs can coregulate a single cell wall gene (Figure 5), suggesting a structured transcriptional homeostasis in a TRN for cell wall components and wood biosynthesis.

We next used the TF-GFP fusion approach to identify which of the 25 (Figure 5, highlighted green) cell wall component genes (Figure 2, step 5) are the direct targets of the nine TFs (Figure 5, highlighted yellow) to reveal the fourth and the bottom layer of the TRN.

TF-GFP Fusion Proteins Retain the Transregulation Activity of the TFs for Members of the PtrMYB, PtrNAC, and PtrWBLH Families

We tested whether the nine GFP-tagged TFs retain the natural transactivation ability. As before, each tagged TF-GFP (*pUC19-35S-TF-sGFP*) and the untagged TF (*pUC19-35S-Ptr-MYB021-35S-sGFP*) were independently overexpressed in SDX protoplasts. The transfected protoplasts were characterized by RT-qPCR for the transcript abundances of three genes randomly selected from those regulated by the tested TF. For example, for *PtrNAC105*, which activates *PtrCesA4*, *PtrCesA7*, and *PtrCAld5H2* (all >2-fold)

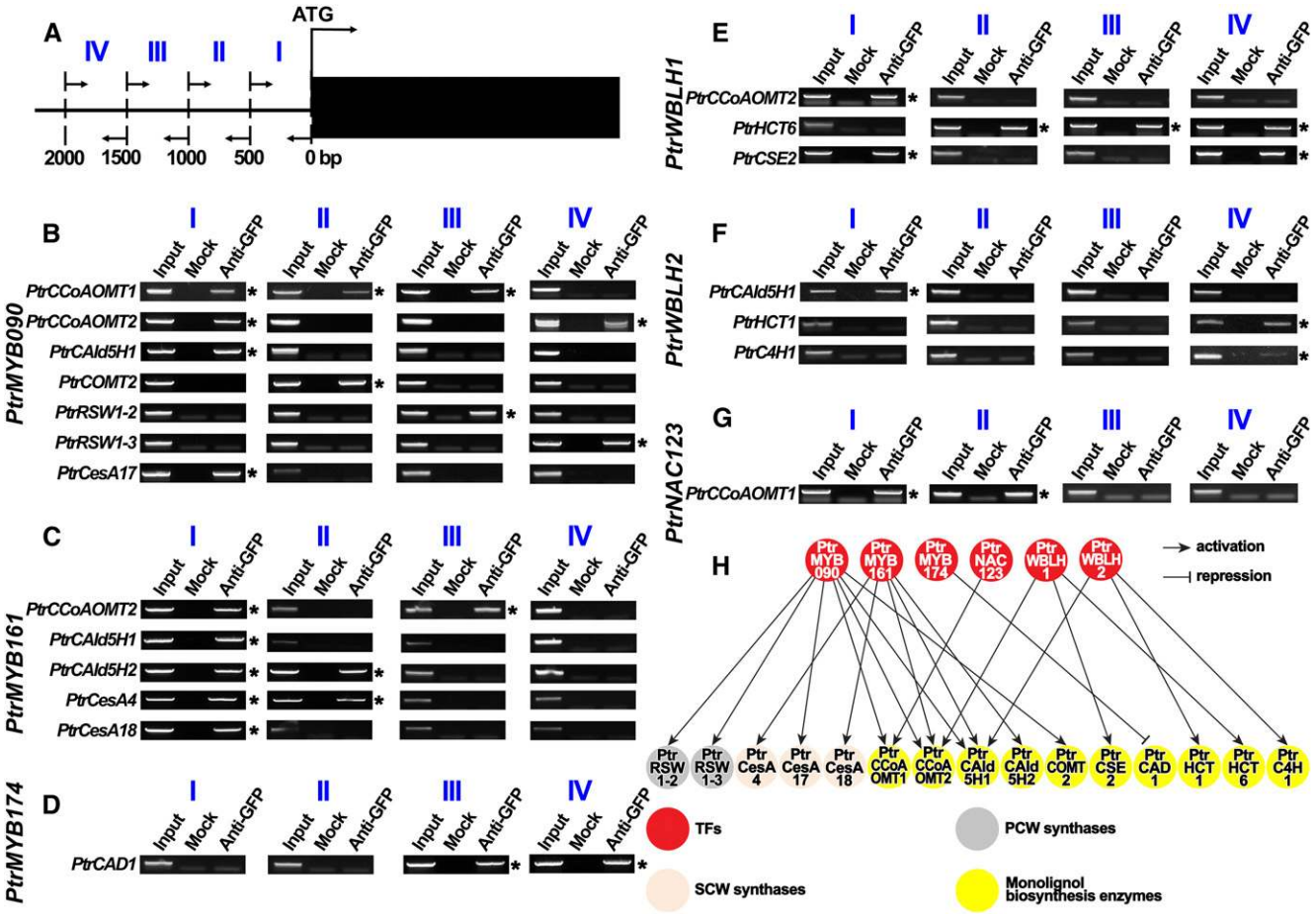

Figure 6. Characterization of TF–DNA Regulatory Interactions between the Third-Layered TFs and Their Regulated Cell Wall Biosynthetic Genes.

(A) Locations of the promoter sequences amplified by PCR following the ChIP assays, as described in Figure 3. The accurate locations of the promoter sequences tested in ChIP-PCR are shown in Supplemental Figure 6.

(B) to **(G)** ChIP assays showed that the direct regulation of PtrMYB090 **(B)**, PtrMYB161 **(C)**, PtrMYB174 **(D)**, PtrWBLH1 **(E)**, PtrWBLH2 **(F)**, and PtrNAC123 **(G)** regulate 15 cell wall genes based on TF–promoter interactions. Four promoter fragments of each target gene were amplified by PCR following ChIP assays. Input, mock, and anti-GFP are PCR reactions using the chromatin preparations before immunoprecipitation, immunoprecipitated with preimmune serum and immunoprecipitated with anti-GFP antibody, respectively. Four independent biological replicates for each ChIP assay were performed, and the results of one biological replicate are presented. A TF–DNA interaction is considered true when at least three of the four biological replicates are positive. The negative results and control for the ChIP-PCR assays of PtrMYB090, PtrMYB161, PtrMYB174, PtrWBLH1, PtrWBLH2, and PtrNAC123 are shown in Supplemental Figure 7.

(H) The network depicts how six TFs directly regulate 15 cell wall biosynthetic genes. The genes are categorized into four functional groups shown by different colors: red for TFs, ivory for secondary cell wall (SCW) synthases, gray for primary cell wall (PCW) synthases, and yellow for monolignol biosynthesis enzymes. Arrows indicate the positive protein–DNA regulatory interactions, and the blunt line indicates a negative protein–DNA regulatory interaction.

and represses *PtrPAL2* (<0.8-fold; Figure 5, Supplemental Data Set 8), we tested and compared the transcriptional regulatory effects of PtrNAC105 and PtrNAC105-GFP on the expression of *PtrCesA4*, *PtrCesA7*, and *PtrPAL2* (Supplemental Figure 3C). For each of the nine tested TFs, the GFP-tagged and untagged proteins similarly activated or repressed the selected cell wall genes (Supplemental Figures 3C to 3K). We then used the TF-GFP system to identify the direct regulators of the 25 cell wall component genes (Figure 5, highlighted in green).

PtrMYB090, PtrMYB161, PtrMYB174, PtrNAC123, PtrWBLH1, and PtrWBLH2 Are Direct Targets of PtrMYB021 and PtrMYB074 and Directly Regulate 15 Monolignol and Primary and Secondary Cell Wall Cellulose Biosynthesis Genes

We overexpressed each of the nine TF-GFPs in SDX protoplasts and analyzed the transfected protoplasts by anti-GFP antibody ChIP as we described in (Figures 3 and 4; Li et al., 2014b). Four chromatin fragments (I to IV; Figure 6A; Supplemental Figure 6) in the ~2-kb promoter of each of the 25 cell wall component genes were PCR amplified for ChIP assays. Six (PtrMYB090, PtrMYB161, PtrMYB174, PtrNAC123, PtrWBLH1, and PtrWBLH2) of the nine TFs were found to directly bind to the promoter of at least one of 15 (out of 25) cell wall genes at single or multiple sites (Figures 6B to 6G; Supplemental Figure 7), establishing 20 direct TF–DNA interactions (Figure 6H). PtrMYB090 and PtrMYB161 directly regulate multiple cellulose synthase genes and multiple monolignol biosynthetic pathway genes (Figures 6B, 6C, and 6H), whereas PtrMYB174, PtrNAC123, PtrWBLH1, and PtrWBLH2 only directly regulate monolignol genes (Figures 6D to 6H). Of the 20 direct TF–DNA interactions regulating the 15 cell wall genes, 19 interactions have not previously been reported. The interaction between PtrNAC123 and PtrCCoAOMT1 (Figure 6G) was reported for a homologous interaction between AtSND2 (a homolog of PtrNAC123) and AtCCoAOMT1 in a Y1H-based Arabidopsis root TRN (Taylor-Teeples et al., 2015). The 15 cell wall component genes directly transregulated by the six third-layer TFs are effector genes of the TRN for wood formation.

A PtrSND1-B1–Mediated Quantitative Hierarchical TRN for Wood Formation

We established a four-layer PtrSND1-B1–mediated TRN that consists of 57 TF–DNA regulatory interactions (Supplemental Data Set 9) between 18 TFs and 27 cell wall biosynthetic genes (Figure 7). Nearly all these ChIP-identified interactions (56/57) result in the upregulation of the target gene expression, suggesting that this TRN is mainly involved in an activation program for xylem cell wall biosynthesis in wood formation. We also quantified the regulatory effect of TF–DNA interactions in SDX protoplasts overexpressing each TF using RNA-seq and RT-qPCR (Supplemental Data Sets 2, 3, and 8; Figure 5). We next tested whether the regulatory effects of these protoplast-inferred TF–DNA interactions take place in planta, using transgenic *P. trichocarpa* plants downregulated for key TFs in the TRN.

Transgenic *P. trichocarpa* Validates the Regulatory Effects of Protoplast-Inferred TRN

We previously reported that ~90% of the protoplast-inferred PtrSND1-B1–DNA interactions tested were validated for their regulatory effects in vivo in the SDX of transgenic *P. trichocarpa*, including those between PtrSND1-B1 and *PtrMYB021* and between PtrSND1-B1 and *PtrMYB074* (Lin et al., 2013). To continue the in vivo validation of the TRN, we downregulated the expression of *PtrMYB021* and *PtrMYB074* in differentiating xylem of *P. trichocarpa* using RNA interference (RNAi) (Figure 2, step 6). A xylem-specific promoter of the *Ptr4CL3* monolignol gene (4CLXP; Wang et al., 2014a) was used to drive the RNAi inverted repeat sequences that target the *PtrMYB021* or *PtrMYB074* transcripts. The transgene constructs *4CLXP-small interfering RNA-PtrMYB021* and *4CLXP-small interfering RNA-PtrMYB074* were transformed into *P. trichocarpa* (see Methods; Song et al., 2006; Wang et al., 2014a, 2018). Twelve independent *PtrMYB021* RNAi lines were generated, and three lines with the lowest *PtrMYB021* transcript levels (Supplemental Figure 8A) were selected for further characterization. Similarly, from nine independent *PtrMYB074* RNAi lines, we selected three lines with the lowest *PtrMYB074* expression (Supplemental Figure 8B).

Using the SDX protoplast system, we demonstrated that PtrMYB021 directly activates eight cell wall biosynthetic genes (Figure 3B) and 10 TF genes (Figure 4B). In the three selected *PtrMYB021* RNAi lines (Supplemental Figure 8A), transcript levels of the eight cell wall biosynthetic genes in the SDX tissue were all reduced (Figure 8A). The expression of 80% (8/10) of the 10 TF targets of PtrMYB021 was also reduced in these *PtrMYB021* RNAi lines (Figure 8B). Overall, ~90% (16/18) of the protoplast-inferred direct targets of PtrMYB021 were downregulated in transgenics where the expression of *PtrMYB021* was suppressed.

We next characterized the selected transgenic *PtrMYB074* RNAi lines (Supplemental Figure 8B) to validate the regulatory effects of PtrMYB074 on its seven direct cell wall biosynthesis targets and 10 direct TF targets inferred by the protoplast system. The transgenics revealed that the expression of all seven cell wall biosynthesis genes (Figure 8C) and 80% of the 10 target TF genes (Figure 8D) was downregulated in response to *PtrMYB074* suppression. Similar to PtrMYB021, the regulatory effects of ~90% (15/17) of the protoplast-inferred TF–DNA interactions for PtrMYB074 were validated in the transgenics. We further selected *PtrMYB090*, a third-layer TF and a common direct target of PtrMYB021 and PtrMYB074 (Figure 7), for validation of the regulatory effects of PtrMYB090 in transgenics (Figure 2, step 6). PtrMYB090 directly regulates seven cell wall component genes (Figure 7). We designed an artificial microRNA (amiRNA) that specifically targets the *PtrMYB090* transcript and prepared the transgene construct *4CLXP-miRNA-PtrMYB090* for transformation in *P. trichocarpa* (Shi et al., 2010a; Wang et al., 2018). Nine independent transgenic lines were generated, and three with the lowest *PtrMYB090* transcript levels were selected for characterization (Supplemental Figure 8C). We quantified the transcript abundance of the seven cell wall component genes in the selected transgenic lines and found that all seven genes exhibited reduced transcript expression compared with controls (Figure 8E).

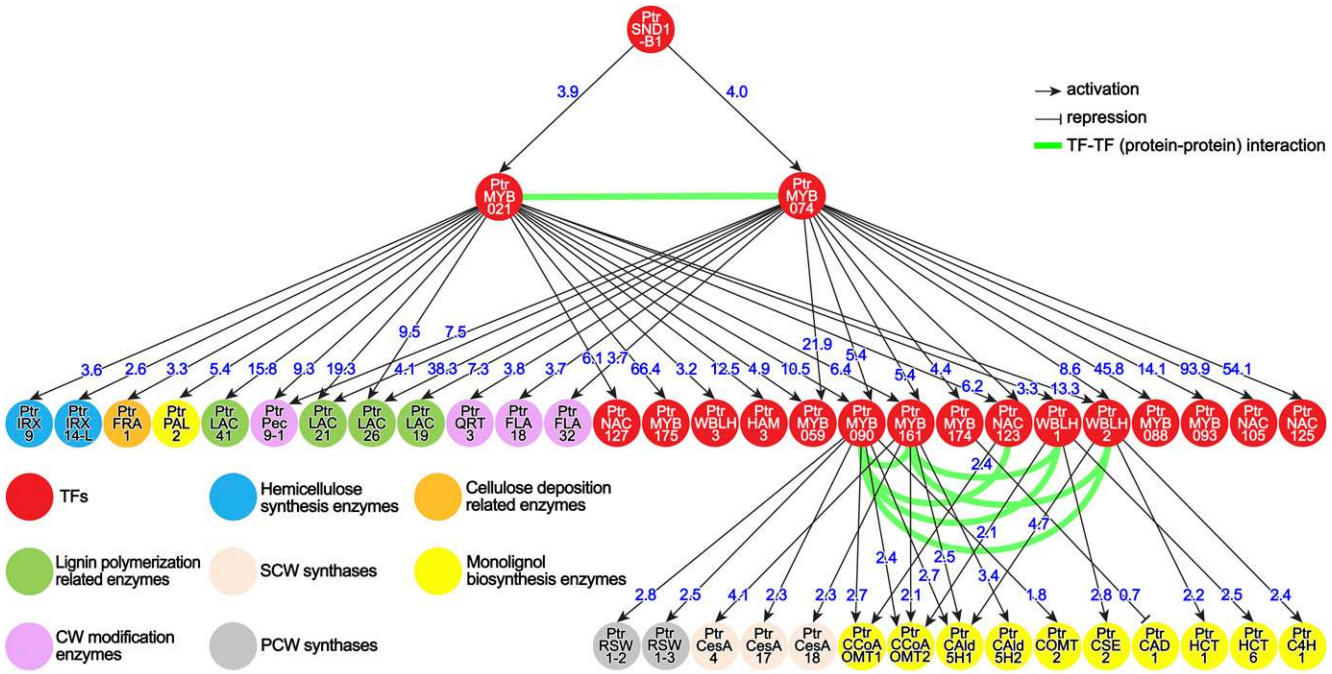

Figure 7. Four-Layered PtrSND1-B1–Mediated TRN Depicting Transcriptional Regulation of Cell Wall Biosynthesis in *P. trichocarpa* SDX.

The 18 TF and 27 cell wall (CW) biosynthetic genes (gene IDs and their annotations are shown in Supplemental Data Set 9) are connected by direct TF–DNA interactions (black lines) in this TRN. Ptr-SND1-B1 is at the top (first layer) of this TRN. The second layer of the TRN consists of *PtrMYB021* and *PtrMYB074* based on Lin et al. (2013). Twenty-seven direct targets of *PtrMYB021* and *PtrMYB074* are presented in the third layer, according to ChIP assays coupled with RNA-seq. The 27 direct targets include 15 cell wall biosynthetic genes and 12 TF genes. PtrMYB021 and PtrMYB074 share eight common direct targets, including three cell wall biosynthetic genes (*PtrLAC21*, *PtrLAC26*, and *PtrPec9-1*) and five TF genes (*PtrMYB059*, *PtrMYB090*, *PtrMYB161*, *PtrNAC123*, and *PtrWBLH2*). In the forth layer, 15 cell wall biosynthetic genes are directly regulated by six TFs (*PtrMYB090*, *PtrMYB161*, *PtrMYB174*, *PtrWBLH1*, *PtrWBLH2*, and *PtrNAC123*). Black lines indicate regulatory protein–DNA interactions. The number on each black line represents fold change of the downstream targets induced by the upstream TF overexpression. Arrows indicate positive regulation (activation), and the blunted line indicates negative regulation (repression). Green lines and curved lines represent TF-TF (protein–protein) interactions. PCW, primary cell wall; SCW, secondary cell wall.

All the regulatory effects discussed above were estimated by RT-qPCR and normalized against the internal 18S ribosomal RNA (rRNA). To verify these effects, three internal reference genes (18S rRNA, actin, and tubulin) were used to characterize six randomly selected TF-direct target sets. We found nearly identical levels of target gene repression based on the expression of these three internal genes (Supplemental Figure 9), supporting the reliability of the identified effects (Figure 8). In addition, we showed that, based on the expression of the three reference genes, the transcript levels of the PtrMYB074-specific targets (e.g., *PtrFLA18* and *PtrFLA32*) in the PtrMYB021-RNAi lines were not significantly different from those in the wild-type control (Supplemental Figure 10). This suggests that the identified transcriptional effects of PtrMYB074 on its targets were not influenced by PtrMYB021. Similarly, the identified transcriptional effects of PtrMYB021 were not induced by PtrMYB074, based on the insignificant difference in the transcript levels of PtrMYB021's targets (e.g., *PtrFRA1* and *PtrIRX9*) between the PtrMYB074-RNAi lines and the wild type (Supplemental Figure 10).

Together, our results showed that 90% of the tested regulatory effects of PtrMYB021, PtrMYB074, and PtrMYB090 inferred by the TRN (Figure 7) are consistent with those in the intact SDX tissues of the transgenics (Figure 8). The results are consistent with our previous findings (Lin et al., 2013), demonstrating that our SDX protoplast–based transregulation system in combination with quantitative transcriptome analysis and ChIP are efficient in revealing wood-forming TF–DNA regulatory networks.

The ChIP-Based TRN Reveals Novel TF–TF (Protein–Protein) Interactions in Regulating Wood Formation

Growth and developmental processes, such as wood formation, are complex and regulated at many levels (Li et al., 2012; Lin et al., 2013, 2017; Wang et al., 2018). Our PtrSND1-B1–based TRN demonstrated that the second-layer TFs (Figure 7), PtrMYB021 and PtrMYB074, directly regulated many common targets (Figures 3 and 4). The coregulation suggests that PtrMYB021 and PtrMYB074 interact to cooperatively bind to the same *cis*-regulatory motifs of their common targets for transregulation. PtrMYB021 and PtrMYB074 bound to the same gene promoter fragment I of *PtrLAC21* and *PtrPec9-1* (Figures 3B and 3C; outlined in Figures 9A to 9G). Similarly, they bound to the same promoter fragment of *PtrMYB161* (fragment II; Figures 4B, 4C, and 9A to 9G) and *PtrWBLH2* (fragment I; Figures 4B, 4C, and 9A). Further tests were performed to explore whether PtrMYB021 and PtrMYB074 interact for TF-DNA binding.

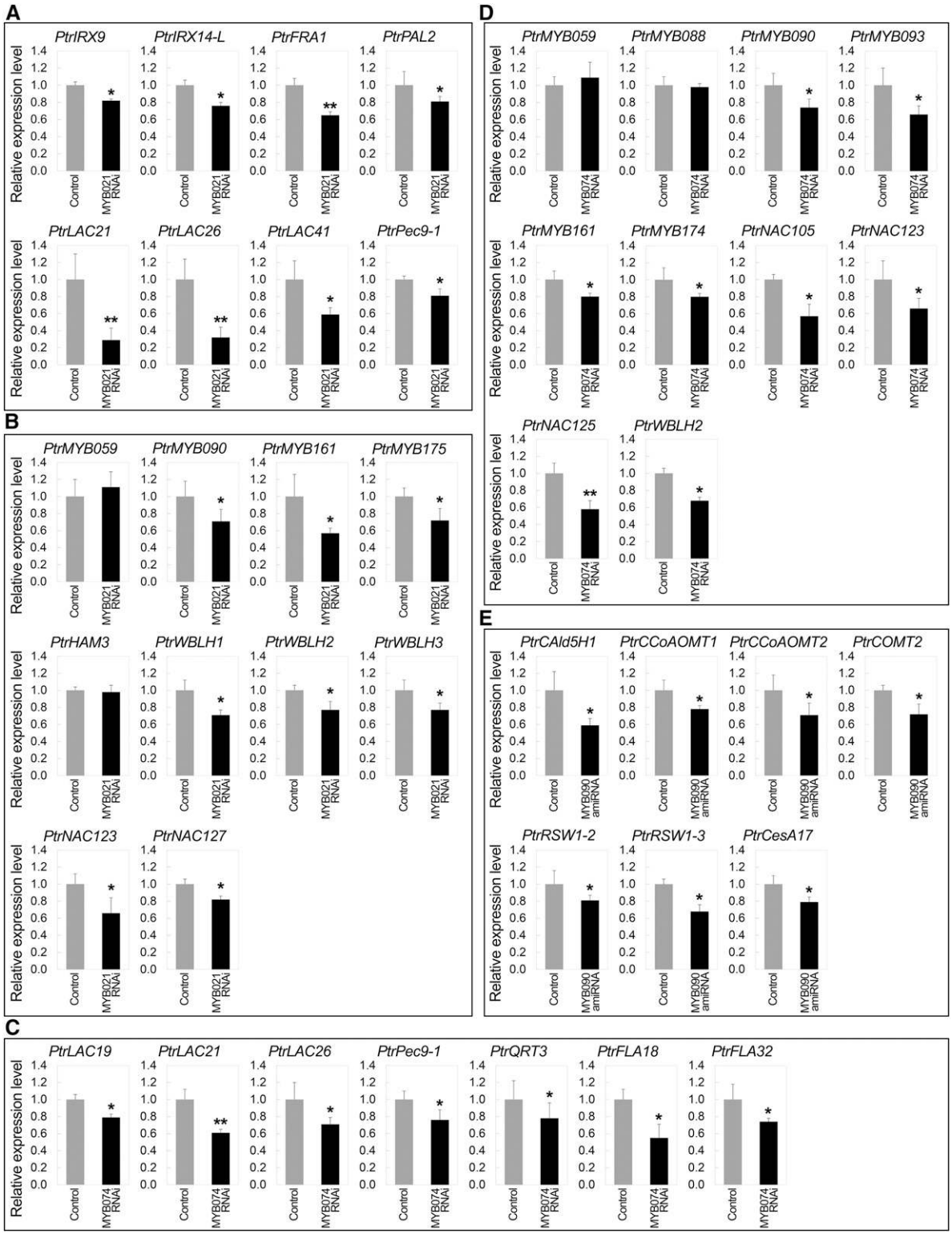

Figure 8. Validation of Direct Regulation of *PtrMYB021*, *PtrMYB074*, and *PtrMYB090* in Stable Transgenic *P. trichocarpa*.

The direct target genes of *PtrMYB021*, *PtrMYB074*, and *PtrMYB090* derived from ChIP assays (shown in Figure 7) were verified by RT-qPCR for their downregulated expression in SDX of stable transgenic *P. trichocarpa* by knocking down *PtrMYB021*, *PtrMYB074*, or *PtrMYB090*.

We performed Y2H assays and confirmed a strong interaction between PtrMYB021 and PtrMYB074 (Figure 9A1). For further confirmation of this interaction in vivo, BiFC assays were performed in *P. trichocarpa* SDX protoplasts. We constructed PtrMYB074-YFP^C (PtrMYB074 fused to the C terminus of yellow fluorescent protein [YFP; amino acids 175 to 239]) and PtrMYB021-YFP^N (PtrMYB021 fused to the N terminus of YFP [amino acids 1 to 174]) and cotransfected them together with the H2A-1-mCherry nuclear marker to the protoplasts. BiFC validated the formation of the PtrMYB021-PtrMYB074 dimer as demonstrated by a positive YFP signal, which colocalized with mCherry in the nucleus (Figure 9A2). The positive BiFC interaction was further verified using three types of negative controls: (1) coexpression of one of the interacting TFs (PtrMYB021-YFP^N) with YFP^C did not give YFP signal (Figure 9A3); (2) coexpression of one of the interacting TFs (PtrMYB021-YFP^N) with a noninteracting TF in the TRN (PtrSND1-B1-YFP^C; Figure 9A4) did not yield YFP signal; and (3) coexpression of one of the interacting TFs (PtrMYB021-YFP^N) with a TF involved in another complex (e.g., YFP^N-PtrNAC123) also did not produce YFP signal (Figure 9A5). These negative controls confirmed the interaction specificity between PtrMYB021 and PtrMYB074. We then used the same three types of negative controls for all subsequent BiFC assays (Figures 9A3 to 9G3, 9A4 to 9G4, and 9A5 to 9G5).

For TFs in the third layer of the TRN, ChIP showed that PtrMYM090 and PtrNAC123 both bind to the promoter fragments I and II of *PtrCCoAOMT1* (Figures 6B, 6G, and 9B). Y2H validated the protein–protein interaction between PtrMYM090 and PtrNAC123 (Figure 9B1), and BiFC confirmed the dimerization of these two TFs in the nucleus of *P. trichocarpa* SDX cells (Figure 9B2). The PtrMYB090-PtrNAC123 interaction is specific, indicated by the results of three negative controls (Figures 9B3 to 9B5).

The third-layer TFs, PtrMYB090, PtrMYB161, and PtrWBLH1, can all bind to the promoter fragment I of *PtrCCoAOMT2* (Figures 6B, 6C, 6E, and 9C to 9E). Y2H further confirmed strong pairwise interactions (Figures 9C1 to 9E1) between these three TFs. BiFC supported the formation of all three possible dimeric protein complexes, PtrMYB090-PtrMYB161 (Figure 9C2), PtrMYB161-PtrWBLH1 (Figure 9D2), and PtrMYB090-PtrWBLH1 (Figure 9E2), in the nucleus. Each dimerization is specific, as revealed by the negative controls (Figures 9C3 to 9C5, 9D3, 9D5, 9E3, and 9E5). The three protein pairs may exist as individual pairs or as combinations of pairs in transregulating *PtrCCoAOMT2* expression. The identification of all three protein pairs may also suggest a ternary protein complex of PtrMYB090-PtrMYB161-PtrWBLH1 for the transregulation of a monolignol pathway gene.

ChIP further indicated that PtrMYB090, PtrMYB161, and PtrWBLH2 may cooperatively transregulate another monolignol pathway gene, *PtrCAld5H1* (Figure 7), because these three TFs bind to a common promoter fragment (fragment I) of the gene (Figures 6B, 6C, 6F, 9C, 9F, and 9G). Between these three TFs, Y2H verified the formation of all three possible pairwise protein–protein interactions, that is, PtrMYB090-PtrMYB161 (Figure 9C1), PtrMYB161-PtrWBLH2 (Figure 9F1), and PtrMYB090-PtrWBLH2 (Figure 9G1). BiFC authenticated the formation (Figures 9C2, 9F2, and 9G2) and specificity (Figures 9C3 to 9C5, 9F3 to 9F5, and 9G3 to 9G5) of these protein–protein interactions in the SDX cell nucleus. The results suggest the participation of these dimers or a PtrMYB090-PtrMYB161-PtrWBLH2 trimer in transregulating *PtrCAld5H1* expression.

The ChIP-based direct TF–DNA interaction network allows accurate prediction of specific TF–TF protein interactions that can be validated by Y2H and BiFC (Figure 9). In this PtrSND1-B1–directed TRN, we identified seven such TF–TF (protein–protein) interactions (Figure 7). These interactions represent new knowledge of a combined TF–DNA and TF–TF regulatory state in a gene expression network for secondary cell wall synthesis in wood formation.

DISCUSSION

We integrated an SDX protoplast system (Lin et al., 2013, 2014, 2017; Li et al., 2014b) with transcriptome and chromatin binding analyses to construct a four-layer quantitative wood formation TRN. This TRN has PtrSND1-B1 as its highest level regulator (Figure 7). PtrSND1-B1 induces 57 specific direct TF–DNA interactions to regulate the expression of 27 effector genes for cell wall component and wood biosynthesis. All genes in this TRN (Figure 7) were coexpressed in both vessel and fiber cells in SDX (Supplemental Data Set 10), suggesting a functional role of the TRN in these wood-forming cell types.

The 57 direct TF–DNA interactions were authenticated by ChIP using a GFP fusion version of the TF, and all TF-GFP fusions retained the transregulation activity of the cognate TF (Figures 3, 4, and 7; Supplemental Figure 3). All 57 direct TF–DNA interactions were quantified using RNA-seq or RT-qPCR. We tested 42 of the 57 direct interactions in transgenic *P. trichocarpa* and validated the transregulation effects of ~90% of the tested interactions in SDX (Figure 8). The transient system reported here could be useful for constructing quantitative TRNs for other species recalcitrant to stable transformation. This PtrSND1-B1 TRN revealed knowledge of TF functions with transregulatory specificity for wood formation.

Figure 8. (continued).

(A) and **(B)** Transcript abundances of ChIP-PCR–verified cell wall biosynthetic genes **(A)** and TF genes **(B)** in *PtrMYB021* transgenic lines and the wild type (control).

(C) and **(D)** Transcript abundances of ChIP-PCR verified cell wall biosynthetic genes **(C)**, and ChIP-PCR verified TF genes **(D)** in wild-type (control) and *PtrMYB074* transgenic lines.

(E) Transcript abundances of ChIP-PCR–verified cell wall biosynthetic genes in *PtrMYB090* transgenics. For each target gene, the average transcript abundance of three biological replicates of the wild-type (control) plants was set as 1. Error bars represent 1 SE of three biological replicates. Asterisks represent significant differences from the wild-type trees, determined using Student's *t* test (*P < 0.05; **P < 0.01). The expression of *PtrMYB059* and *PtrMYB090* in *PtrMYB021* transgenics, and *PtrMYB059* and *PtrMYB088* in *PtrMYB074* transgenics, showed no significant change in gene expression compared with the wild-type trees.

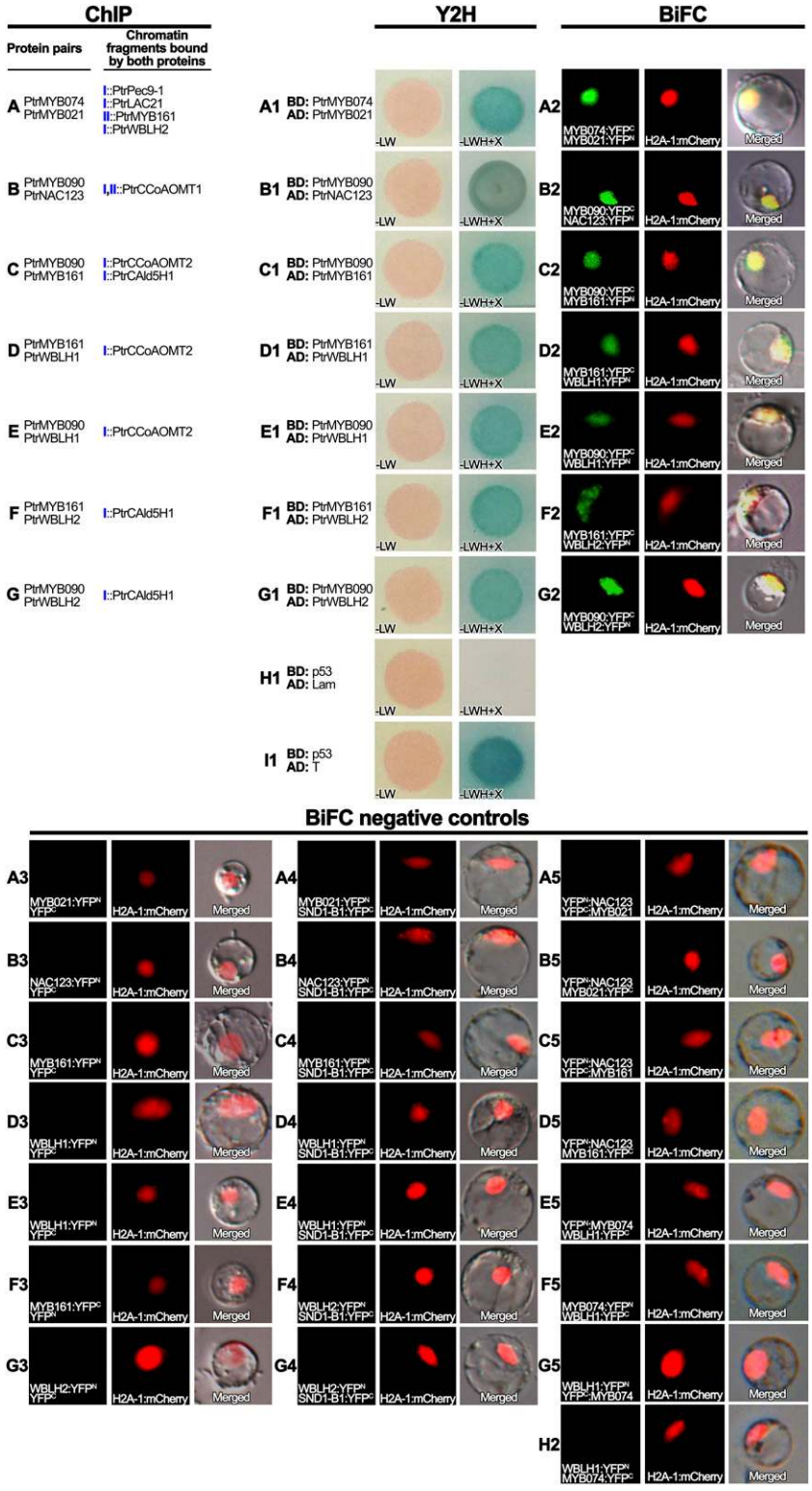

Figure 9. Y2H and BiFC Demonstrate That TF Pairs Binding to the Same Promoter Fragments May Interact with Each Other.

TF pairs (PtrMYB021 and PtrMYB074, PtrMYB090 and PtrNAC123, PtrMYB090 and PtrMYB161, PtrMYB161 and PtrWBLH1, PtrMYB090 and PtrWBLH1, PtrMYB161 and PtrWBLH2, and PtrMYB090 and PtrWBLH2) bind to the same promoter fragments, as indicated by ChIP-PCR in Figures 3, 4, and 6.

The TRN provides information for the comparison of regulation in herbaceous plant systems.

SND1-Mediated TRN in *P. trichocarpa* Is Distinct from That in Arabidopsis

The closest functional homolog of *PtrSND1-B1* in Arabidopsis is *AtSND1*, which is a single gene in the Arabidopsis *SND1* family (Zhong et al., 2006; Li et al., 2012; Lin et al., 2013, 2017). We deduced an AtSND1-mediated TRN (Figure 10) for secondary wall formation based on experimentally generated data so far from studies of more than 470 TFs in 31 plant species in the PubMed database (Supplemental Data Set 1). Like in our PtrSND1-B1 TRN (Figure 7), all pairwise TF–DNA interactions in the AtSND1 TRN are direct (Figure 10), and the interactions were quantified for trans-regulatory effects (Supplemental Data Sets 2, 3, and 8). We then compared the two SND1-mediated TRNs (Figures 7 and 10) with demonstrated regulatory paths and effects.

These two TRNs are distinct (Figures 7 and 10). PtrSND1-B1 directly regulates 10 TF genes (two shown in Figure 7; Lin et al., 2013), whereas AtSND1 directly regulates 14 TF genes (Figure 10; Supplemental Data Set 11). Among all these TFs, only one is commonly regulated by the two SND1 homologs (Figures 7 and 10). This TF is a *MYB*, *PtrMYB021* in *P. trichocarpa* or *AtMYB46* in Arabidopsis, which are the two *MYB* homologs in these two species sharing the highest amino acid sequence similarity (72%), based on sequences producing significant alignments in the Arabidopsis Information Resource online database (Altschul et al., 1997). Our previous study showed that PtrSND1-B1 directly regulates three cell wall biosynthetic genes, *PtrLAC26* (*Potri.010G183600*), *PtrLAC19* (*Potri.008G073800*), and *PtrLAC18* (*Potri.008G073700*; Lin et al., 2013), whereas Arabidopsis AtSND1 directly regulates a different set of nine cell wall component genes (Figure 10; Supplemental Data Set 11). The identification of these direct TF and cell wall gene targets of either PtrSND1-B1 or AtSND1 (Zhong et al., 2010a) was exclusive because target genes were screened on a genome-wide basis. Therefore, at the SND1 level, the SND1 TRNs in *Populus* and in Arabidopsis share only one common regulatory path—the SND1-mediated activation of *PtrMYB021* in *Populus* or *AtMYB46* in Arabidopsis.

The homologous SND1-MYB regulation was also identified in maize (*Zea mays*) and rice (*Oryza sativa*; Zhong et al., 2011). The maize SND1 (ZmSND1) directly regulates *ZmMYB109* (Zhong et al., 2011), a homolog of *PtrMYB021* and *AtMYB46*. In rice, OsNAC29, the homolog of PtrSND1-B1 and AtSND1, directly regulates OsMYB46 (Zhong et al., 2011), a homolog of *PtrMYB021* and *AtMYB46*. This specific SND1-MYB regulation may be a conserved higher level regulation of secondary cell wall formation in plants. After the SND1-MYB regulation, the MYB's regulatory paths become distinct in different species (Supplemental Data Set 11).

The Functions of the Two MYB Homologs PtrMYB021 and AtMYB46 Are Species Specific

In *P. trichocarpa*, PtrMYB021 directly regulates eight cell wall component genes and 10 TF genes (Figures 3, and 4,7), whereas in Arabidopsis AtMYB46 directly regulates 12 cell wall component genes and 17 TF genes (Figure 10). Among these 20 cell wall gene regulatory interactions, PtrMYB021 and AtMYB46 share only two common targets—a PAL gene (*PtrPAL2* and its Arabidopsis homolog *AtPAL1*) and a hemicellulose biosynthetic pathway gene (*PtrIRX14-L*, Potri.005G141500 and *AtIRX14-L*, AT5G67230) (Figure 10). For the 27 TF gene regulations, the two MYB homologs share four common direct targets (Figure 10). In the Arabidopsis TRN, they are *AtMYB52*, *AtBLH2*, *AtBLH3*, and *AtBLH6*. In the *P. trichocarpa* TRN, the four common targets are represented by six TFs. These six TFs are *PtrMYB090*, *PtrMYB161*, *PtrMYB175*, *PtrWBLH1*, *PtrWBLH2*, and *PtrWBLH3*, where *PtrMYB090*, *PtrMYB161*, and *PtrMYB175* are phylogenetically paired homologs and are most similar to *AtMYB52*.

Overall, the SND1-MYB regulation leads to 18 immediate downstream regulatory paths mediated by PtrMYB021 in *P. trichocarpa* (Figure 7) and 29 by AtMYB46 in Arabidopsis (Figure 10), with only six overlapping paths (Figure 10; Supplemental Data Set 11), suggesting species specificity for the SND1-MYB regulations. We next discovered that another SND1-MYB regulation, the PtrSND1-B1 and *PtrMYB074* direct interaction, is more woody dicot specific.

PtrMYB074 Encodes a Woody Dicot–Specific MYB

Phylogenetic analysis of 69 plant species (Phytozome 11; https://phytozome.jgi.doe.gov/) showed that all MYB homologs sharing

Figure 9. (continued).

(A) to **(G)** Y2H demonstrated that these TF pairs can physically interact with each other. Each bait and prey pair were coexpressed in yeast cells and selected on the SD/–Leu/–Trp (–LW) medium: **(A)** AD-PtrMYB021 and BD-PtrMYB074, **(B)** BD-PtrMYB090 and AD-PtrNAC123, **(C)** BD-PtrMYB090 and AD-PtrMYB161, **(D)** BD-PtrMYB161 and AD-PtrWBLH1, **(E)** BD-PtrMYB090 and AD-PtrWBLH1, **(F)** BD-PtrMYB161 and AD-PtrWBLH2, and **(G)** BD-PtrMYB090 and AD-PtrWBLH2).

(A1) to **(G1)** Protein–protein interaction of each pair was validated by the growth of the transformants on SD/–Leu/–Trp/–His/–X-Gal (–LWHX) medium.

(A2) to **(G2)** BiFC demonstrated that ChIP-validated pairs of TFs heterodimerizes with each other. Each pair of TF proteins, PtrMYB021-YFP^N and PtrMYB074-YFP^C **(A2)**, PtrMYB090-YFP^C and PtrNAC123-YFP^N **(B2)**, PtrMYB090-YFP^C and PtrMYB161-YFP^N **(C2)**, PtrMYB161-YFP^C and PtrWBLH1-YFP^N **(D2)**, PtrMYB090-YFP^C and PtrWBLH1-YFP^N **(E2)**, PtrMYB161-YFP^C and PtrWBLH2-YFP^N **(F2)**, and PtrMYB090-YFP^C and PtrWBLH2-YFP^N **(G2)**, coexpressed into SDX protoplasts gave a positive BiFC signal for heterodimerization, which are colocalized with H2A-1-mCherry signal in the nucleus. As negative controls, transformation of single TF-YFP^N with YFP^C alone (**[A3]** to **[G3]**), with a noninteracting TF (SND1-B1-YFP^C) (**[A4]** to **[G4]**), or TFs in other complexes (**[A5]** to **[H2]**), did not give any YFP signals.

(H1) and **(I1)** Negative control was indicated by BD-53/AD-Lam **(H1)**, whereas positive growth was confirmed using the positive control BD-53/AD-T **(I1)**.

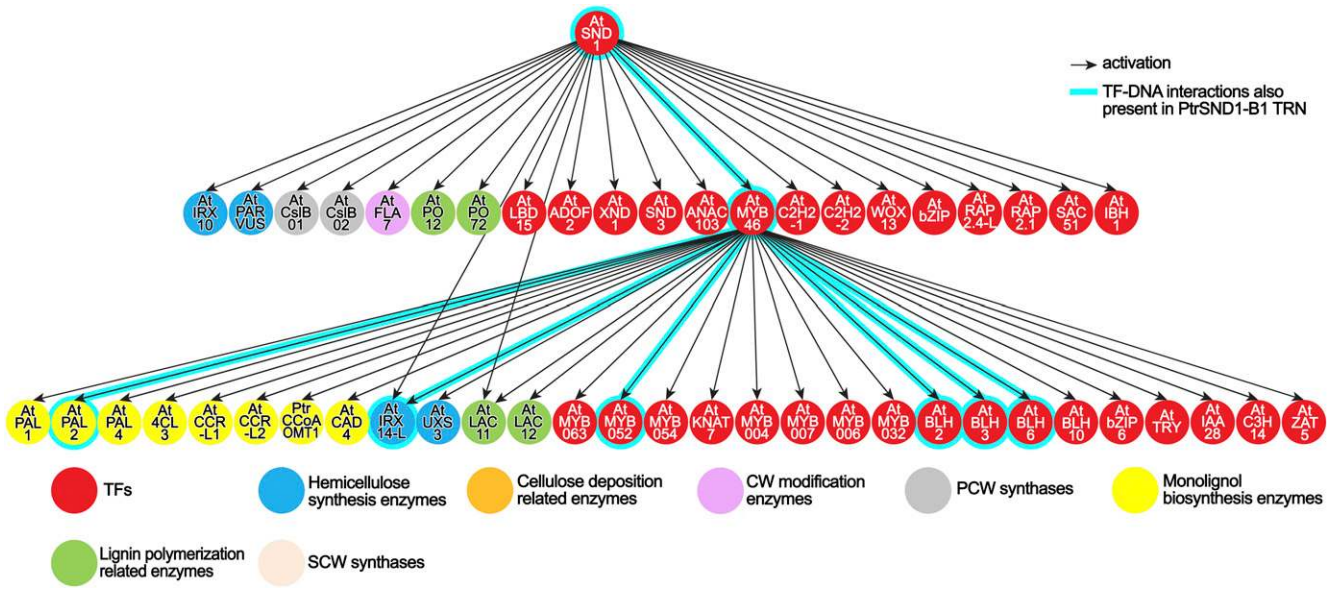

Figure 10. Three-Layered Network Encompassed by AtSND1 and AtMYB46 Regulating Cell Wall Biosynthetic Genes in Arabidopsis

Based on studies using inducible assays, electrophoretic mobility shift assay, Y1H, or ChIP assays (Zhong et al., 2010a; Zhong and Ye, 2012), 14 TF and 7 cell wall biosynthetic genes were identified as the direct targets of AtSND1, and 17 TF and 12 cell wall biosynthetic genes are direct targets of AtMYB46. Using these TF–DNA interactions, a three-layered hierarchical TRN directed by AtSND1 and AtMYB46 was constructed for Arabidopsis stem cell wall biosynthesis. Black lines indicate the regulatory TF–target regulation through protein–DNA interactions. Cyan shading indicates TF–DNA interactions also present in the *P. trichocarpa* SND1-B1 TRN. CW, cell wall; SCW, secondary cell wall.

high levels of amino acid sequence similarity with *PtrMYB074* are from dicots, particularly woody dicots (63.1 to 100%, clade I; Supplemental Figure 11; Supplemental Data Set 12). *MYB*s from herbaceous monocots (clade III; Supplemental Figure 11) exhibit low protein similarity (51.5 to 59.8%) with *PtrMYB074*. This phylogeny does not include any Arabidopsis *MYB*s (Supplemental Figure 11; Supplemental Data Set 12). However, there are four Arabidopsis *MYB*s having low amino acid sequence similarity with *PtrMYB074*. They are *AtMYB7* (AT2G16720), *AtMYB17* (AT3G61250), *AtMYB35* (At3G28470), and *AtMYB50* (AT1G57560), showing similarities of 33.2, 36.1, 35.3, and 32.9% with *PtrMYB074*, respectively. Such low similarities suggest that these *AtMYB*s are functionally divergent from *PtrMYB074*.

AtMYB7 regulates flavonol biosynthesis in Arabidopsis leaves by direct transregulation of genes associated with early steps in the flavonol pathway (Fornalé et al., 2014). Mutation and transgenesis in *AtMYB7* had no effect on monolignol gene expression, nor did it affect lignin content or composition (lignin syringyl [S]: guaiacyl [G] ratios) in Arabidopsis stems (Fornalé et al., 2014). Similarly, mutation of *AtMYB17* (also known as *LMI2* [*LATE MERISTEM IDENTITY 2*]; Pastore et al., 2011) and *AtMYB35* (also known as *TDF1* [*TAPETAL DEVELOPMENT AND FUNCTION* 1]; Zhu et al., 2008) also did not induce any phenotypic changes in the secondary cell wall in Arabidopsis stems. Arabidopsis does not have MYBs with functions homologous to PtrMYB074. Therefore, the PtrSND1-B1–regulated PtrMYB074 expression and its associated TF–target DNA interactions (Figure 7) are likely to be specific for cell wall biosynthesis in wood formation.

The *Populus* Wood Formation TRN and the Arabidopsis Root Xylem TRN Have Distinct Regulatory Functions

Recently, an Arabidopsis root xylem cell wall TRN was constructed based on Y1H screening of interactions between 467 TFs and promoters of 45 genes implicated in Arabidopsis cell wall formation (Taylor-Teeples et al., 2015). The screening resulted in a five-layer TRN that included 209 TFs mediating 617 TF–DNA interactions, of which three were validated by ChIP (Taylor-Teeples et al., 2015). We compared this Arabidopsis TRN with our PtrSND1-B1–mediated wood formation TRN.

The PtrSND1-B1 TRN's 18 TFs (Figure 7) have 28 unique sequence homologs in the Arabidopsis genome (Supplemental Data Set 13). Nine (AtMYB46, AtMYB85, AtBLH6, AtNAC75, AtSND2, AtBLH3, AtHAM1, ATMYB32, and AtSND3; Supplemental Data Set 13) of these 28 homologs are in the five-layer Arabidopsis root xylem cell wall TRN (Taylor-Teeples et al., 2015). These nine TFs directly mediate 16 interactions (Supplemental Data Set 14) in the Arabidopsis root TRN, where only one interaction, that is, between AtSND2 and AtCCoAOMT1, has a homologous interactive pair (PtrNAC123 and PtrCCoAOMT1; Figure 7) in the PtrSND1-B1–mediated wood TRN. In addition, the Arabidopsis root cell wall TRN does not include AtSND1 (Taylor-Teeples et al., 2015), the counterpart of PtrSND1-B1. The Arabidopsis root TRN appears to lack many key regulatory interactions specialized for xylem secondary cell wall formation in wood development.

The different regulations of the PtrSND1-B1 wood TRN and the Arabidopsis root TRN may lead to the drastic divergence in cell

wall composition and physiological functions between stem wood in trees and roots in Arabidopsis. Lignin in the wood of angiosperm trees, such as *P. trichocarpa*, consists of ~70% S and ~30% G monomers, with a trace amount of *p*-hydroxyphenyl units (Lu et al., 2013; Wang et al., 2014a, 2018), whereas Arabidopsis root lignin has ~5% S, ~90% G, and ~5% *p*-hydroxyphenyl monomers (Naseer et al., 2012). The polysaccharide components of wood cell walls are biosynthesized from monosaccharides of mainly Glc (~40%), Xyl(~17%), and uronic acid (11%), with trace amounts of Ara (~0.5%) and rhamnose (~0.5%; Lu et al., 2013). This cell wall composition is considerably different from that in Arabidopsis roots, where uronic acid (~30%) and Ara (~20%) are the predominant monomers and Glc, Xyl, Gal, and rhamnose each account for ~10% of the total monosaccharides (Diet et al., 2006). Variations in cell wall composition in distinct organ types may be associated with certain functional specialization of these organs. Specific cell wall properties in roots may be needed for rapid anisotropic cell expansion to maximize nutrient uptake (Enstone et al., 2003). Cell walls in wood provide a tree stem with the necessary mechanical strength to support the enormous weight of a tree crown (Evert, 2006).

The ChIP-Based TRN Reveals Additional Regulation at the Level of Protein–Protein Interactions

TFs typically work cooperatively and combinatorially to regulate their DNA targets (Müller, 2001; Levine and Tjian, 2003; Hobert, 2008; Lin et al., 2013, 2017). Such regulations suggest involvement of TF–TF protein interactions or binding of TF protein oligomers to specific chromatin sequences for transregulation. Information on interactive protein dimers or complexes is difficult to obtain because there are no rules to infer protein oligomerization based on transcript or protein sequences. A haploid transformation–based Y1H system could test whether two or more prey TFs are needed to activate a target gene promoter (Yang et al., 2017). Because this approach might predict TF–TF protein interactions, it was used to study the regulation of phenylpropanoid biosynthesis in maize (Yang et al., 2017). Twenty-one Y1H-positive TF pairs were selected and further evaluated by Y2H (Yang et al., 2017). Of these 21 pairs, only four pairs were demonstrated to have pairwise interactions (Yang et al., 2017). The approach is useful, despite its low accuracy (19%, 4/21) in the experiment. Perhaps more accurate estimation of TF–protein interactions can be obtained from a TF TRN.

In our TRN, the ChIP assays generate information on the segments of the target gene promoters where a TF protein would directly bind (Figures 3, and 4, 6). Therefore, any two TFs having a common direct promoter target in our TRN are possible interactive partners, particularly those that bind to the same promoter segments. The TRN in Figure 7 reveals seven such TF pairs (Figures 3, and 4, 6, 9), all validated for the pairwise interactions and dimerization by Y2H and BiFC (Figure 9). We suggest that a TF-based TRN, constructed experimentally or computationally, can identify protein–protein interactions that mediate gene transregulation. However, these identified interactions need to be validated for function in vivo.

TF Protein Complexes May Regulate Wood Chemical Composition

The PtrSND1-B1 TRN reveals that while individual TFs can directly activate multiple cell wall component genes, the seven paired TFs we identified (Figure 9) seem to target a few specific monolignol pathway genes (Figure 7). Four such pairs (Figures 9B to 9E) target *CCoAOMT* gene family members and three pairs (Figures 9C, 9F, and 9G) target a single member of the *CAld5H* gene family. In *Populus*, CCoAOMT enzymes are involved more specifically in the biosynthesis of the G type of monolignol subunits in lignin (Ye et al., 1994; Zhong et al., 1998; Li et al., 1999; Wang et al., 2014a). CAld5H is needed for the biosynthesis of the S subunits (Osakabe et al., 1999; Li et al., 2000, 2001; Wang et al., 2012, 2014a, 2018). The proportion of S and G subunits determines lignin composition and chemical linkages (Freudenberg, 1959, 1965; Ralph et al., 1997, 2008; Wang et al., 2014a, 2018) affecting physical and chemical properties of cell walls and thus the plant's ability to defend against pests and pathogens (Vance et al., 1980; Dixon, 2001; Dixon et al., 2002; Pomar et al., 2004; Bhuiyan et al., 2009; Dhillon et al., 2015; Foster et al., 2015). The lignin S:G subunit ratio determines wood processing efficiency for pulp/paper, biofuel, and biomaterial productions (Hu et al., 1999; Chiang, 2002; Li et al., 2003, 2014a; Ragauskas et al., 2006; Chen and Dixon, 2007; Lu et al., 2013; Wang et al., 2018). The TRN suggests that six dimeric (Figures 9B to 9G) TF protein complexes are direct regulators of lignin properties and structures. Three pairwise interactions, PtrMYB090-PtrMYB161, PtrMYB161-PtrWBLH1, and PtrMYB090-PtrWBLH1, may suggest the formation of a ternary complex (Chen et al., 2011) of PtrMYB090-PtrMYB161-PtrWBLH1, which may regulate the CCoAOMT level for G subunit biosynthesis. Similarly, the other three dimers, PtrMYB090-PtrMYB161, PtrMYB161-PtrWBLH2, and PtrMYB090-PtrWBLH2, may suggest a PtrMYB090-PtrMYB161-PtrWBLH2 trimer in regulating the CAld5H abundance for S subunit formation. These eight regulators (dimers and trimers) may cooperatively or combinatorially mediate the biosynthesis of specific types of lignin. Such mediation may be necessary at different stages of cell wall differentiation for proper metabolism, development, and adaptation. The specific roles of these TF protein–complex regulators and their TFs are unknown. The lack of TF mutants in any forest tree species limits our current understanding of such roles. Genome editing–based mutations of individual or combinations of the TFs in the TRN of woody plants, such as *P. trichocarpa* (Li et al., 2018), offer the potential to resolve these questions and to elucidate the complex roles and specific regulatory mechanisms associated with wood formation.

A Quantitative TRN Is Essential for Predictive Modeling of the Regulation of Plant Metabolism

TF–DNA interactions in TRNs are often highly combinatorial, with specifically structured cascades and regulatory paths (Figure 7). How individual interactions and their combinatorial effects control the expression of effector genes are sufficiently complex that mathematical models are required for utilization of the TRN. All individual TF–DNA interactions in a TRN need to be quantified to develop a mathematical framework. The work reported here

introduces a useful system for developing such quantitative TRNs. A mathematical model can be used to predict how to increase or reduce the expression of specific effector genes by perturbing key TFs in combinations to improve wood properties and to ameliorate biotic and abiotic stresses threatening forest tree growth, reproduction, and adaptation.

Limitations of the Present Approach

ChIP combined with transactivation assays in plant protoplasts represents one of the most efficient approaches to identify TF–target gene regulations. However, if an interaction is dependent on cofactors that are regulated spatiotemporally or by specific developmental/environmental conditions, protoplasts may not reveal such an interaction. Untransfected protoplasts in the TF transregulation assays may also mask the detection of weakly downregulated target genes (Lin et al., 2014). TF–TF protein interactions (complexes) may incur alterations to their target specificity distinct from the individual TFs. Conversely, induced regulatory effects of an individual TF on a target gene may represent only part of the effects if the target gene is combinatorially regulated by multiple TFs. In the present study, TF binding sites were assayed within 2-kb upstream of the coding region, a range typical for TF–DNA interactions. TFs that bind further upstream or downstream of this region were unexploited. Potential feedback regulation of a TF transgene on its endogenous counterpart could not be analyzed because the transgenes were expressed in far excess of the endogenous genes (e.g., *PtrMYB074* transgene abundance was 276-fold higher than that of the endogenous gene). As for the effector genes, only currently known wood cell wall biosynthetic genes were included, which may not be exclusive. While limitations to the current approach exist, the present study describes a comprehensive base network as a starting point to which additional regulatory components can be incorporated in future studies.

CONCLUSION

We have begun to uncover the quantitative knowledge of transcriptional regulation in wood formation through the analysis of a PtrSND1-B1–directed hierarchical TRN expressed during xylem differentiation of *P. trichocarpa*. The PtrSND1-B1 TRN includes two hemicellulose genes in the third layer and 15 cellulose and monolignol genes in the bottom layer (Figure 7). There are at least 54 genes with known or putative functions for the direct biosynthesis of the three major wood cell wall components (Suzuki et al., 2006; Kumar et al., 2009; Shi et al., 2010b, 2017; Vanholme et al., 2013; Wang et al., 2014a, 2018). A complete hierarchical and functional TRN in wood formation needs further study to gain systems understanding of how the regulation is transduced to all cell wall component genes to affect wood phenotypes (Wang et al., 2018). The wood TRN can be extended to include other regulations, such as for biotic and abiotic stresses. Such TRNs can reveal the extent to which plant–environment interactions give rise to alternative phenotypes (phenotypic plasticity) or whether there is a high degree of homeostasis determined by the TF–target gene interactions.

Genetic regulation of wood formation is best studied in woody or forest tree species because of their abundance and specialization in secondary xylem, or wood. The well-annotated genome sequence of *P. trichocarpa* as a model woody plant offers the best opportunity to integrate genomics and epigenomics for a comprehensive understanding of TRNs and their regulation at different levels for wood formation. Such understanding is possible without using mutants or stable transgenics. The system developed here (Figure 2) can be exploited to better understand other complex processes in plant metabolism and adaptation.

METHODS

Plant Materials

Black cottonwood (*Populus trichocarpa*) plants (genotype Nisqually-1) were grown and maintained in a greenhouse following Song et al. (2006). Clonal propagation was performed using cut branches (~10 cm) rooted in water. The rooted branches were planted in a mixture of 50:50 Miracle-Gro soil (Scotts Miracle-Gro Products) and Metro-Mix 200 (Sun Gro) in 16-cm pots that were kept at 17 to 26°C, 16-h-light/8-h-dark cycle with supplemented lighting (LU600W/PSL/T/E40; Lucalox) of ~300 μE m^{-2} s^{-1} (Song et al., 2006). The tissues of healthy ~3- to 9-month-old plants were used for stable transformation, RNA isolation, and SDX protoplast isolation.

Laser Microdissection

The stem-differentiating fiber cells, vessel cells, or a mixture of all three cell types (fiber, vessel, and ray) were collected from 6-month-old, greenhouse-grown *P. trichocarpa* using an LMD7000 laser microdissection microscope (Leica) according to Chen et al. (2014). Total RNA from the three cell type samples was isolated and analyzed by RT-qPCR following Chen et al. (2014); Supplemental Data Set 15.

Gene Cloning

Total RNA from SDX, differentiating phloem, mature leaves, juvenile shoots, and mature roots of *P. trichocarpa* was individually isolated using the RNeasy plant RNA isolation kit (Qiagen). One microgram of total RNA from each tissue was reverse transcribed to coding DNA (cDNA; Omniscript RT kit; Qiagen). The full-length coding sequences of *PtrWBLH1*, *PtrWBLH2*, *PtrWBLH3*, *PtrNAC125*, *PtrNAC127*, *PtrMYB021*, *PtrMYB074*, *PtrMYB088*, *PtrMYB090*, *PtrMYB161*, *PtrMYB174*, and *PtrMYB175* were amplified from the cDNA of differentiating xylem. *PtrNAC123* was amplified from the cDNA of juvenile shoots. *PtrMYB059*, *PtrHAM3*, and *PtrNAC105* were amplified from the cDNA of differentiating phloem. *PtrMYB093* was amplified from the cDNA of mature leaves. Primers for gene cloning are listed in Supplemental Data Set 15. The amplified coding sequences were assembled into *pENTR-D-TOPO* vectors and verified by sequencing.

Constructs for Transient Overexpression of TFs in SDX Protoplasts

The coding sequence of each TF was subcloned from the *pENTR-D-TOPO* vectors into *pUC19-35S-RfA-35S-sGFP* (Li et al., 2012) using LR reactions to replace the original *RfA* sequence, generating transient overexpression constructs *pUC19-35S-TF-35S-sGFP* for 17 TFs (*PtrWBLH1*, *PtrWBLH2*, *PtrWBLH3*, *PtrNAC105*, *PtrNAC123*, *PtrNAC125*, *PtrNAC127*, *PtrHAM3*, *PtrMYB021*, *PtrMYB059*, *PtrMYB074*, *PtrMYB088*, *PtrMYB090*, *PtrMYB093*, *PtrMYB161*, *PtrMYB174*, and *PtrMYB175*).

Constructs for ChIP Assays Coupled with TF Overexpression

The coding sequences of 11 TFs (*PtrMYB021*, *PtrMYB074*, *PtrMYB090*, *PtrMYB161*, *PtrMYB174*, *PtrMYB175*, *PtrWBLH1*, *PtrWBLH2*, *PtrWBLH3*, *PtrNAC105*, and *PtrNAC123*) were amplified using primers (Supplemental Data Set 15), restriction digested, and ligated into *pUC19-35S-GFP* (Li et al., 2014b) to generate *pUC19-35S-TF-GFP* for each of 11 TFs.

Constructs for Y2H

The coding sequences of *PtrMYB090* and *PtrMYB161* and the N terminus (1 to 471 bp) of *PtrMYB074* were amplified, digested, and individually cloned into the bait vector *pGBKT7*. The coding regions of *PtrMYB021*, *PtrMYB161*, *PtrNAC123*, *PtrWBLH1*, and *PtrWBLH2* were cloned into the prey vector *pGADT7 AD* (Clontech). Primer sequences are listed in Supplemental Data Set 15.

Constructs for BiFC

PtrMYB074, *PtrMYB090*, *PtrMYB161*, *PtrWBLH1*, and *PtrWBLH2* coding sequences without stop codons were individually cloned into *pENTR-D-TOPO* vectors. *PtrMYB074*, *PtrMYB090*, *PtrMYB161*, *PtrWBLH1*, and *PtrWBLH2* coding sequences without stop codons were transferred into *pUGW2* to generate the *35S-MYB074-YFP^C*, *35S-MYB090-YFP^C*, *35S-MYB161-YFP^C*, *35S-MYB161-YFP^N*, *35S-WBLH1-YFP^N*, and *35S-WBLH2-YFP^N* constructs for BiFC. Similarly, the coding regions of *PtrMYB021* and *PtrNAC123* were cloned into *pUGW0* using LR reactions, resulting in *35S-MYB021-YFP^N* and *35S-MYB161-YFP^N*.

Constructs for RNAi Suppression

Type I RNAi constructs targeting the individual knockdown of *PtrMYB021* and *PtrMYB074* were designed and assembled following Wang et al. (2018). RNAi fragments were designed to be sequence specific to the individual target genes and confirmed by BLAST against the *P. trichocarpa* genome sequence. The RNAi constructs (*pBI121-4CLXP*) originated from the *pBI* binary vector backbone with replacement of the 35S promoter by the *Ptr4CL3* xylem-specific promoter. RNAi fragments of *PtrMYB021* and *PtrMYB074* were amplified using primers (Supplemental Data Set 15), restriction digested, and assembled with a 600-bp GUS spacer (GL) to form an antisense:GL:sense fragment as RNAi transgene sequence and cloned into an intermediate plasmid (*pCR2.1*; Li et al., 2011). The assembled RNAi transgene fragments, confirmed by sequencing, were digested and cloned into the *pBI121-4CLXP* plasmid to replace the original GUS sequence (Wang et al., 2018). The constructs were introduced into *Agrobacterium tumefaciens* C58 for plant transformation (Song et al., 2006).

Constructs for amiRNA-Mediated Gene Silencing

The amiRNA transgene of *PtrMYB090* was assembled based on the transcript of *PtrMIR408* (Wang et al., 2018). The *PtrMYB090* amiRNA sequence (TATCGTAGAACTCAATCGGGC) was designed using the online program WMD (http://wmd.weigelworld.org) and the genome of *P. trichocarpa* v1.0 (JGI). To minimize off-target sites, the no off-target algorithm was activated in the WMD program to design the *PtrMYB090* amiRNA sequence. The designed *PtrMYB090* amiRNA sequence was amplified and cloned into the *pBI121*-based amiRNA expression binary vector with the *Ptr4CL3* promoter, following Shi et al. (2010b) and Wang et al. (2018). For plant transformation, the *pBI121*-based *PtrMYB090* amiRNA construct was transformed into *A. tumefaciens* C58 (Song et al., 2006).

SDX Protoplast Preparation and Transformation

The subcellular localization, transient overexpression, ChIP, and BiFC assays were performed using SDX protoplasts (Lin et al., 2014). Plasmid DNA for protoplast transfection was prepared using caesium chloride density-gradient ultracentrifugation (Lin et al., 2014). The preparation and transfection of SDX protoplasts were performed as described in Lin et al. (2014), with three modifications. The mannitol concentration in mannitol-magnesium solution was adjusted down to 0.4 M from 0.5 M, and 0.1 M Glc was added to the W5 solution, which increased the transfection efficiency. Ampicillin (50 μg mL^{-1}) was added during the protoplast incubation to inhibit bacterial growth.

Subcellular Localization of PtrMYB021 and PtrMYB074

The constructs *pUC19-35S-MYB021-sGFP* and *pUC19-35S-MYB074-sGFP* were expressed in SDX protoplasts for subcellular localization. The nuclear marker *pUC19-35S-H2A-Cherry* was cotransfected with each construct to mark the subcellular localization of the PtrMYB proteins. After a 12-h incubation, fluorescence in SDX protoplasts was analyzed using an LSM 710 laser-scanning microscope (Zeiss). Excitation and emission wavelengths were 488 nm and 492 to 543 nm, respectively, for GFP and 561 nm and 582 to 662 nm, respectively, for mCherry.

BiFC

BiFC plasmids for each tested combination of TFs were cotransfected with H2A-1-mCherry into SDX protoplasts (Figures 9A2 to 9G2). For each experiment, three types of negative controls were included (Figures 9A3 to 9H2). Three biological replicates (independent isolation of SDX protoplasts and plasmid transfection) were performed for each combination of TFs and the negative controls. After incubation for 12 h, SDX protoplasts were collected, and at least 12 individual protoplast cells for each combination of the protein fusions were examined under a DM6 B microscope (Leica). One representative image for each combination is shown (Figures 9A2 to 9G4). For fluorescence detection, the excitation wavelength and the emission wavelength were 515 and 525 nm, respectively, for YFP and 561 nm and 598 to 648 nm, respectively, for mCherry.

Transient Overexpression of TFs in SDX Protoplasts

Plasmid DNA (*pUC19-35S-TF-35S-sGFP*) for the transient overexpression of 17 TFs (*PtrWBLH1*, *PtrWBLH2*, *PtrWBLH3*, *PtrNAC105*, *PtrNAC123*, *PtrNAC125*, *PtrNAC127*, *PtrHAM3*, *PtrMYB021*, *PtrMYB059*, *PtrMYB074*, *PtrMYB088*, *PtrMYB090*, *PtrMYB093*, *PtrMYB161*, *PtrMYB174*, and *PtrMYB175*) in SDX protoplasts were prepared using caesium chloride density-gradient ultracentrifugation (Lin et al., 2014). Transfected protoplasts were incubated in 100 $\times$ 15-mm^2 Petri dishes for 7 h, collected by centrifugation at 300*g* for 3 min at room temperature, and frozen in liquid nitrogen. Total RNA was isolated from the protoplasts using an RNeasy plant RNA isolation kit and analyzed by RNA-seq (*PtrMYB021* and *PtrMYB074*) and qRT-PCR (all 17 TFs).

ChIP Assays

pUC19-35S-TF-GFP constructs of nine TFs (*PtrMYB021*, *PtrMYB074*, *PtrMYB090*, *PtrMYB161*, *PtrMYB174*, *PtrMYB175*, *PtrWBLH1*, *PtrWBLH2*, and *PtrNAC123*) were individually transfected into SDX protoplasts following our procedures (Lin et al., 2014, 2017). TF-GFP–transfected SDX protoplasts (10^7 to 10^8 cells) were resuspended in washing/incubation buffer with 1% (v/v) formaldehyde and incubated for 10 min for cross-linking at room temperature. The cross-linked SDX protoplasts were washed with cold washing/incubation buffer and glycine, resuspended in lysis buffer, and sonicated using a sonifier 250 (Branson) to

generate DNA–protein fragments that range from 0.2 to 2 kb. The solution with DNA–protein fragments was diluted 10-fold into ChIP dilution buffer (Li et al., 2014b) and held at 4°C. The solution was divided into two parts: one part with anti-GFP antibodies (1:100 dilution) (10 to 15 μg, ab290; Abcam) for 24 h and another part with rabbit IgG (ab171870; Abcam) Dynabeads with protein G (10003D; Thermo Fisher Scientific) were added to the solution and held for 4 h at 4°C to isolate the antibody-DNA-TF complex. The complexes were rinsed using low salt washing buffer followed by a high-salt washing buffer, LiCl washing buffer, and TF buffer (Li et al., 2014b) to remove nonspecific binding complexes. Immunoprecipitated protein-DNA complexes were eluted using prewarmed elution buffer and reverse cross-linked using 5 M NaCl at 65°C overnight. The separated DNA was isolated using a QIAprep Miniprep (Qiagen) to produce the immunoprecipitation samples. Input and mock samples were collected following Li et al. (2014b). All reagents and buffers were prepared based on (Li et al., 2014b). For the ChIP-PCR experiments, 200 ng of DNA was used (25-μL volumes, 25 to 36 cycles). Four biological replicates (four independent batches of SDX protoplast transfections for four independent ChIP experiments) were performed (Supplemental Data Set 16).

Y2H Assays

Y2H assays were performed according to the Matchmaker Gold Y2H System (Clontech). Prepared bait and prey plasmids (Figures 9A1 to 9G1) were cotransformed into the Y2HGold yeast strain and selected on synthetic dropout-agar plates lacking Leu and Trp (SD/–Leu/–Trp). Strong positive interactions were tested on synthetic dropout-agar plates lacking Leu, Try, and His and supplemented with 40 mg/mL X-α-Gal (SD/–Leu/–Trp/–His/X-α-Gal, TDO/X), and incubated for 3 to 5 d at 30°C. Interaction between PtrMYB090 and PtrNAC123 was weaker and was detected using SD plates lacking leucine and tryptophan, supplemented with 40 mg/mL X-α-Gal (SD/–Leu/–Trp/X-α-Gal, DDO/X), and incubated for 3 to 5 d at 30°C.

RT-qPCR

SDX protoplasts overexpressing TFs were collected at 7 h by centrifugation at 500*g* for 3 min at room temperature. Total RNAs were isolated from the SDX protoplast pellet using an RNeasy plant RNA isolation kit and treated with RNase-free DNase (Qiagen) to remove genomic DNA and residual plasmid. The quality of the extracted RNA was examined by gel electrophoresis and UV spectrogram scanning. Total RNA (80 ng) was reverse transcribed, using TaqMan reverse transcription reagents (Applied Biosystems). RT-qPCR was conducted with a 7900HT sequence detection system (Applied Biosystems), following our published procedures (Shi et al., 2010b). At least three technical replicates were performed for each assay, and the average transcript level was normalized to the expression of 18S rRNA (Schmittgen and Livak, 2008).

Transcriptome Analyses of the Transfected SDX Protoplasts and Identification of DEGs

SDX protoplasts individually overexpressing *PtrMYB021*, *PtrMYB074*, and *sGFP* were analyzed by RNA-seq with three biological replicates per gene. Total RNA from each sample (750 ng) was extracted for library construction using the TruSeq RNA sample preparation kit (Illumina). The quality and concentration of libraries were verified using a 2100 bioanalyzer using high-sensitivity DNA assay chips (Agilent). Different index adaptors were used for the libraries, and they were pooled for sequencing in one lane (HiSeq 2500). Sequencing reads were mapped to *P. trichocarpa* genome v2.2 and v3.0 (Phytozome; www.phytozome.com) using TOPHAT (Trapnell et al., 2009). The normalized raw counts were determined following (Lin et al., 2013). Differentially expressed genes (FDR < 0.05; fold change > 2 or fold change < 0.8) induced by the overexpression of *PtrMYB021* and *PtrMYB074* were identified by EdgeR (Robinson et al., 2010), by comparison with the transcript abundance in *sGFP* (control).

GO Functional Enrichment Analysis

GO for the differentially expressed genes were annotated using the g:Profiler Web server (http://biit.cs.ut.ee/gprofiler/; Reimand et al., 2016). The *P. trichocarpa* GO functional enrichment analysis in the g:Profiler web server is based on the Ensemble Genome (http://www.ensembl.org) annotation for the *P. trichocarpa* gene set. The statistical significance of functional enrichment (g:Profiler) is calculated for the *PtrMYB021* and *PtrMYB074* activated genes using $P < 0.05$ using Fisher's exact test.

Phylogenetic Analyses

The sequences of PtrMYB074 homologs were extracted from the genome of 69 plant species (Phytozome 11; https://phytozome.jgi.doe.gov/). The multiple sequence alignment of PtrMYB074 homologs (>60% amino acid sequence similarity with PtrMYB074) were performed using the ClustalW program using the default settings. A phylogenetic tree based on the alignment was constructed using MEGA6.0 by the neighbor-joining method with the bootstrap test replicated 1000 times.

Statistical Analysis

All RT-qPCR were statistically analyzed using Student's *t* test. The statistical analyses for RNA-seq are based on the transcript fold change between different samples and an appropriate FDR using the EdgeR package. All GO enrichment analyses in this study were performed using Fisher's exact test.

Accession Numbers

Sequence data from this article can be found in *P. trichocarpa* genome v3.0 (Phytozome; www.phytozome.com) under the accession numbers described in Supplemental Data Sets 2, 3, and 9. The RNA-seq data were submitted to the Gene Expression Omnibus database (www.ncbi.nlm.nih.gov/geo/) under accession number GSE81077.

Supplemental Data

Supplemental Figure 1. Identification of two PtrSND1-B1 (Secondary Wall NAC Domain) direct targets, PtrMYB021 and PtrMYB074, that are preferentially expressed in SDX.

Supplemental Figure 2. Genes regulated by PtrMYB021 and PtrMYB074 in SDX protoplasts at 7 h after transfection.

Supplemental Figure 3. Transcriptional regulation abilities of the GFP-tagged and untagged TFs from the TRN.

Supplemental Figure 4. Graphical representation of the promoters of PtrMYB021- and PtrMYB074-targeted cell wall biosynthetic genes analyzed by ChIP-PCR.

Supplemental Figure 5. Graphical representation of the promoters of PtrMYB021- and PtrMYB074-targeted transcription factor genes analyzed by ChIP-PCR.

Supplemental Figure 6. Graphical representation of the promoters of cell wall biosynthetic genes regulated by the third-layer TFs, which are tested in ChIP-PCR assays.

Supplemental Figure 7. Negative results and control of ChIP-PCR assays for detecting the protein–DNA interaction between nine third-layer TFs and their 25 regulated cell wall biosynthetic genes.

Supplemental Figure 8. Expression of PtrMYB021, PtrMYB074, and PtrMYB090 in the knockdown transgenic *P. trichocarpa* plants.

Supplemental Figure 9. Comparison of multiple normalization genes for qRT-PCR.

Supplemental Figure 10. Transcript quantification of nontargeted genes in RNAi transgenic *P. trichocarpa*.

Supplemental Figure 11. Phylogenetic tree of PtrMYB074 homologs (>60% amino acid sequence similarity with PtrMYB074) in plants.

Supplemental Table 1. Significant GO functional classes of 164 DEGs induced by PtrMYB021 overexpression.

Supplemental Table 2. Significant GO functional classes of 135 DEGs upregulated by PtrMYB074.

Supplemental Table 3. GO analysis of the PtrMYB021 overexpression-induced DEGs that are involved in cell wall biosynthesis.

Supplemental Table 4. GO analysis of the PtrMYB074 overexpression-induced DEGs that are involved in cell wall biosynthesis.

Supplemental Data Set 1. Plant transcription factors (476) from 31 plant species that directly regulate secondary cell wall biosynthetic genes.

Supplemental Data Set 2. Functional annotation and classification of the 164 genes induced by PtrMYB021 overexpression.

Supplemental Data Set 3. Functional annotation and classification of the 135 genes induced by PtrMYB074 overexpression.

Supplemental Data Set 4. Transcript abundances of the cell wall biosynthetic genes induced by PtrMYB021 or PtrMYB074 overexpression in four tissues (developing xylem, developing phloem, mature leaf, and juvenile shoot) of *P. trichocarpa*.

Supplemental Data Set 5. Transcript abundances of TFs induced by PtrMYB021 or PtrMYB074 overexpression in four tissues (developing xylem, developing phloem, mature leaf, and juvenile shoot) of *P. trichocarpa*.

Supplemental Data Set 6. TFs that are directly and indirectly regulated by PtrMYB021 or PtrMYB074 in SDX protoplasts.

Supplemental Data Set 7. The 36 cell wall biosynthetic genes whose expression was measured in different batches of SDX protoplasts that are transformed with each of the 15 third-layer TFs.

Supplemental Data Set 8. Transcript abundance changes of 36 cell wall component genes in response to the overexpression of each of the 15 third-layer TFs and 2 second-layer TFs.

Supplemental Data Set 9. Protein–DNA interactions identified by ChIP assays in this study.

Supplemental Data Set 10. SDX cell (fiber cells, vessel cells, and three cell types)–specific expression of the cell wall biosynthetic genes and TF genes in SND1-B1–directed four-layered TRN.

Supplemental Data Set 11. Transcription factor and cell wall biosynthetic genes regulated by AtSND1 and AtMYB46 in Arabidopsis and by PtrSND1-B1 and PtrMYB021 in *P. trichocarpa.*

Supplemental Data Set 12. Amino acid sequence alignment of PtrMYB074 homologs (>60% amino acid sequence similarity with PtrMYB074).

Supplemental Data Set 13. The 28 Arabidopsis protein homologs of 18 TFs in *P. trichocarpa* SDX TRN.

Supplemental Data Set 14. The nine Arabidopsis TFs directly mediating 16 TF–DNA interactions in root TRN.

Supplemental Data Set 15. Primers used in this study.

Supplemental Data Set 16. Biological replicates of the ChIP-PCR assays.

ACKNOWLEDGMENTS

This work was supported by the National Natural Science Foundation of China (grant nos. 31430093 and 31522014); China Postdoctoral Science Foundation (grant 2015M581410); Heilongjiang Postdoctoral Financial Assistance (grant no. LBH-Z15008); and the Innovation Project of State Key Laboratory of Tree Genetics and Breeding (Northeast Forestry University) grant no. A01. We also acknowledge the financial support from the 1000-talents Plan for young researchers from China and Longjiang Young Scholar Program of Heilongjiang Provincial Government (to W.L.), the U.S. Department of Energy (Biological and Environmental Research) (grant no. DE-SC000691 to V.L.C.), Taiwan Ministry of Science and Technology MOST (grant nos. 106-2311-B-002-001-MY2 and 107-2636-B-002-003 to Y.-C.J.L.), the Fundamental Research Funds for the Central Universities of China (grant no. 2572018CL01), and the 111 Project of the Fundamental Research Funds (grant no. B16010).

AUTHOR CONTRIBUTIONS

V.L.C., H.C., J.P.W., W.L., and Y.-C.J.L. designed the research. H.C., J.P.W., H. Liu., H. Li, Y.-C.J.L., R.S., C.Y., J.G., C.Z., Q.L., and W.L. performed the research. H.C., J.P.W., W.L., Y.-C.J.L., R.R.S., and V.L.C. analyzed data. H.C., J.P.W., W.L., H. Liu, Y.-C.J.L., R.R.S., and V.L.C. wrote the article with input from all co-authors.

Received August 20, 2018; revised January 15, 2019; accepted February 7, 2019; published February 12, 2019.

REFERENCES

Albersheim, P., Darvill, A., Roberts, K., Sederoff, R., and Staehelin, A. (2011). Cell walls and plant anatomy. *In* P Albersheim, A Darvill, K Roberts, R Sederoff, and A Staehelin, eds, Plant Cell Walls: From Chemistry to Biology, Garland Science, New York, pp 1–42.

Altschul, S.F., Madden, T.L., Schäffer, A.A., Zhang, J., Zhang, Z., Miller, W., and Lipman, D.J. (1997). Gapped BLAST and PSI-BLAST: A new generation of protein database search programs. Nucleic Acids Res. **25:** 3389–3402.

Berthet, S., Demont-Caulet, N., Pollet, B., Bidzinski, P., Cézard, L., Le Bris, P., Borrega, N., Hervé, J., Blondet, E., Balzergue, S., Lapierre, C., and Jouanin, L. (2011). Disruption of LACCASE4 and 17 results in tissue-specific alterations to lignification of *Arabidopsis thaliana* stems. Plant Cell **23:** 1124–1137.

Bhardwaj, N., Kim, P.M., and Gerstein, M.B. (2010). Rewiring of transcriptional regulatory networks: Hierarchy, rather than connectivity, better reflects the importance of regulators. Sci. Signal. **3:** ra79.

Bhuiyan, N.H., Selvaraj, G., Wei, Y., and King, J. (2009). Gene expression profiling and silencing reveal that monolignol biosynthesis plays a critical role in penetration defence in wheat against powdery mildew invasion. J. Exp. Bot. **60:** 509–521.

Chai, G., Qi, G., Cao, Y., Wang, Z., Yu, L., Tang, X., Yu, Y., Wang, D., Kong, Y., and Zhou, G. (2014). Poplar PdC3H17 and PdC3H18 are direct targets of PdMYB3 and PdMYB21, and positively regulate

secondary wall formation in Arabidopsis and poplar. New Phytol. **203:** 520–534.

Chen, H.C., et al. (2014). Systems biology of lignin biosynthesis in *Populus trichocarpa*: Heteromeric 4-coumaric acid: Coenzyme A ligase protein complex formation, regulation, and numerical modeling. Plant Cell **26:** 876–893.

Chen, F., and Dixon, R.A. (2007). Lignin modification improves fermentable sugar yields for biofuel production. Nat. Biotechnol. **25:** 759–761.

Chen, H.C., Li, Q., Shuford, C.M., Liu, J., Muddiman, D.C., Sederoff, R.R., and Chiang, V.L. (2011). Membrane protein complexes catalyze both 4- and 3-hydroxylation of cinnamic acid derivatives in monolignol biosynthesis. Proc. Natl. Acad. Sci. USA **108:** 21253–21258.

Cheng, C., Yan, K.K., Hwang, W., Qian, J., Bhardwaj, N., Rozowsky, J., Lu, Z.J., Niu, W., Alves, P., Kato, M., Snyder, M., and Gerstein, M. (2011). Construction and analysis of an integrated regulatory network derived from high-throughput sequencing data. PLOS Comput. Biol. **7:** e1002190.

Chiang, V.L. (2002). From rags to riches. Nat. Biotechnol. **20:** 557–558.

Davidson, E.H., et al. (2002). A genomic regulatory network for development. Science **295:** 1669–1678.

Davidson, E.H. (2010). Emerging properties of animal gene regulatory networks. Nature **468:** 911–920.

Deplancke, B., et al. (2006). A gene-centered *C. elegans* protein-DNA interaction network. Cell **125:** 1193–1205.

Deplancke, B., Dupuy, D., Vidal, M., and Walhout, A.J. (2004). A gateway-compatible yeast one-hybrid system. Genome Res. **14:** 2093–2101.

de Souza, A., Hull, P.A., Gille, S., and Pauly, M. (2014). Identification and functional characterization of the distinct plant pectin esterases PAE8 and PAE9 and their deletion mutants. Planta **240:** 1123–1138.

Dhillon, B., et al. (2015). Horizontal gene transfer and gene dosage drives adaptation to wood colonization in a tree pathogen. Proc. Natl. Acad. Sci. USA **112:** 3451–3456.

Diet, A, Link, B, Seifert, G.J., Schellenberg, B., Wagner, U., Pauly, M., Reiter, W.D., and Ringli, C. (2006). he Arabidopsis root hair cell wall formation mutant lrx1 is suppressed by mutations in the RHM1 gene encoding a UDP-L-rhamnose synthase. The Plant Cell **18:** 1630–1641.

Dixon, R.A. (2001). Natural products and plant disease resistance. Nature **411:** 843–847.

Dixon, R.A., Achnine, L., Kota, P., Liu, C.J., Reddy, M.S., and Wang, L. (2002). The phenylpropanoid pathway and plant defence-a genomics perspective. Mol. Plant Pathol. **3:** 371–390.

Enstone, D.E., Peterson, C.A., and Ma, F. (2003). Root endodermis and exodermis: Structure, function, and responses to the environment. J. Plant Growth Regul. **21:** 335–351.

Erwin, D.H., and Davidson, E.H. (2009). The evolution of hierarchical gene regulatory networks. Nat. Rev. Genet. **10:** 141–148.

Evert, R.F. (2006). Xylem: Secondary Xylem and Variations in Wood Structure, *In* Esau's Plant Anatomy. John Wiley & Sons, New York, pp 291–322.

Faraco, M., Di Sansebastiano, G.P., Spelt, K., Koes, R.E., and Quattrocchio, F.M. (2011). One protoplast is not the other! Plant Physiol. **156:** 474–478.

Farnham, P.J. (2009). Insights from genomic profiling of transcription factors. Nat. Rev. Genet. **10:** 605–616.

Fornalé, S., Lopez, E., Salazar-Henao, J.E., Fernández-Nohales, P., Rigau, J., and Caparros-Ruiz, D. (2014). AtMYB7, a new player in the regulation of UV-sunscreens in *Arabidopsis thaliana.* Plant Cell Physiol. **55:** 507–516.

Foster, A.J., Pelletier, G., Tanguay, P., and Séguin, A. (2015). Transcriptome analysis of poplar during leaf spot infection with *Sphaerulina* spp. PLoS One **10:** e0138162.

Freudenberg, K. (1959). Biosynthesis and constitution of lignin. Nature **183:** 1152–1155.

Freudenberg, K. (1965). Lignin: Its constitution and formation from p-hydroxycinnamyl alcohols: Lignin is duplicated by dehydrogenation of these alcohols; intermediates explain formation and structure. Science **148:** 595–600.

Gerstein, M.B., et al. (2010). Integrative analysis of the *Caenorhabditis elegans* genome by the modENCODE project. Science **330:** 1775–1787.

Goicoechea, M., Lacombe, E., Legay, S., Mihaljevic, S., Rech, P., Jauneau, A., Lapierre, C., Pollet, B., Verhaegen, D., Chaubet-Gigot, N., and Grima-Pettenati, J. (2005). EgMYB2, a new transcriptional activator from *Eucalyptus* xylem, regulates secondary cell wall formation and lignin biosynthesis. Plant J. **43:** 553–567.

Goodstein, D.M., Shu, S., Howson, R., Neupane, R., Hayes, R.D., Fazo, J., Mitros, T., Dirks, W., Hellsten, U., Putnam, N., and Rokhsar, D.S. (2012). Phytozome: A comparative platform for green plant genomics. Nucleic Acids Res. **40:** D1178–D1186.

Hägglund, E. (1952). Chemistry of Wood. Academic Press, New York.

Hens, K., Feuz, J.D., Isakova, A., Iagovitina, A., Massouras, A., Bryois, J., Callaerts, P., Celniker, S.E., and Deplancke, B. (2011). Automated protein-DNA interaction screening of *Drosophila* regulatory elements. Nat. Methods **8:** 1065–1070.

Hobert, O. (2008). Gene regulation by transcription factors and microRNAs. Science **319:** 1785–1786.

Hu, W.J., Harding, S.A., Lung, J., Popko, J.L., Ralph, J., Stokke, D. D., Tsai, C.J., and Chiang, V.L. (1999). Repression of lignin biosynthesis promotes cellulose accumulation and growth in transgenic trees. Nat. Biotechnol. **17:** 808–812.

Jin, J., Tian, F., Yang, D.C., Meng, Y.Q., Kong, L., Luo, J., and Gao, G. (2017). PlantTFDB 4.0: Toward a central hub for transcription factors and regulatory interactions in plants. Nucleic Acids Res. **45** (D1): D1040–D1045.

Karpinska, B., Karlsson, M., Srivastava, M., Stenberg, A., Schrader, J., Sterky, F., Bhalerao, R., and Wingsle, G. (2004). MYB transcription factors are differentially expressed and regulated during secondary vascular tissue development in hybrid aspen. Plant Mol. Biol. **56:** 255–270.

Ko, J.H., Kim, W.C., Kim, J.Y., Ahn, S.J., and Han, K.H. (2012). MYB46-mediated transcriptional regulation of secondary wall biosynthesis. Mol. Plant **5:** 961–963.

Ko, J.H., Jeon, H.W., Kim, W.C., Kim, J.Y., and Han, K.H. (2014). The MYB46/MYB83-mediated transcriptional regulatory programme is a gatekeeper of secondary wall biosynthesis. Ann. Bot. **114:** 1099–1107.

Kumar, M., Thammannagowda, S., Bulone, V., Chiang, V., Han, K. H., Joshi, C.P., Mansfield, S.D., Mellerowicz, E., Sundberg, B., Teeri, T., and Ellis, B.E. (2009). An update on the nomenclature for the cellulose synthase genes in *Populus.* Trends Plant Sci. **14:** 248–254.

Lee, T.I., et al. (2002). Transcriptional regulatory networks in *Saccharomyces cerevisiae.* Science **298:** 799–804.

Lee, C., Teng, Q., Zhong, R., Yuan, Y., and Ye, Z.H. (2014). Functional roles of rice glycosyltransferase family GT43 in xylan biosynthesis. Plant Signal. Behav. **9:** e27809.

Legay, S., et al. (2010). EgMYB1, an R2R3 MYB transcription factor from eucalyptus negatively regulates secondary cell wall formation in Arabidopsis and poplar. New Phytol. **188:** 774–786.

Levine, M., and Davidson, E.H. (2005). Gene regulatory networks for development. Proc. Natl. Acad. Sci. USA **102:** 4936–4942.

Levine, M., and Tjian, R. (2003). Transcription regulation and animal diversity. Nature **424:** 147–151.

Li, S., et al. (2018). Histone acetylation cooperating with AREB1 transcription factor regulates drought response and tolerance in *Populus trichocarpa.* Plant Cell.

Li, J.J., and Herskowitz, I. (1993). Isolation of ORC6, a component of the yeast origin recognition complex by a one-hybrid system. Science **262:** 1870–1874.

Li, C., Wang, X., Ran, L., Tian, Q., Fan, D., and Luo, K. (2015). PtoMYB92 is a Transcriptional activator of the lignin biosynthetic pathway during secondary cell wall formation in *Populus tomentosa.* Plant Cell Physiol. **56:** 2436–2446.

Li, L., Osakabe, Y., Joshi, C.P., and Chiang, V.L. (1999). Secondary xylem-specific expression of caffeoyl-coenzyme A 3-O-methyltransferase plays an important role in the methylation pathway associated with lignin biosynthesis in loblolly pine. Plant Mol. Biol. **40:** 555–565.

Li, L., Popko, J.L., Umezawa, T., and Chiang, V.L. (2000). 5-hydroxyconiferyl aldehyde modulates enzymatic methylation for syringyl monolignol formation, a new view of monolignol biosynthesis in angiosperms. J. Biol. Chem. **275:** 6537–6545.

Li, L., Cheng, X.F., Leshkevich, J., Umezawa, T., Harding, S.A., and Chiang, V.L. (2001). The last step of syringyl monolignol biosynthesis in angiosperms is regulated by a novel gene encoding sinapyl alcohol dehydrogenase. Plant Cell **13:** 1567–1586.

Li, L., Zhou, Y., Cheng, X., Sun, J., Marita, J.M., Ralph, J., and Chiang, V.L. (2003). Combinatorial modification of multiple lignin traits in trees through multigene cotransformation. Proc. Natl. Acad. Sci. USA **100:** 4939–4944.

Li, Q., Min, D., Wang, J.P., Peszlen, I., Horvath, L., Horvath, B., Nishimura, Y., Jameel, H., Chang, H.M., and Chiang, V.L. (2011). Down-regulation of glycosyltransferase 8D genes in *Populus trichocarpa* caused reduced mechanical strength and xylan content in wood. Tree Physiol. **31:** 226–236.

Li, Q., Lin, Y.C., Sun, Y.H., Song, J., Chen, H., Zhang, X.H., Sederoff, R.R., and Chiang, V.L. (2012). Splice variant of the SND1 transcription factor is a dominant negative of SND1 members and their regulation in *Populus trichocarpa.* Proc. Natl. Acad. Sci. USA **109:** 14699–14704.

Li, Q., Song, J., Peng, S., Wang, J.P., Qu, G.Z., Sederoff, R.R., and Chiang, V.L. (2014a). Plant biotechnology for lignocellulosic biofuel production. Plant Biotechnol. J. **12:** 1174–1192.

Li, W., Lin, Y.C., Li, Q., Shi, R., Lin, C.Y., Chen, H., Chuang, L., Qu, G.Z., Sederoff, R.R., and Chiang, V.L. (2014b). A robust chromatin immunoprecipitation protocol for studying transcription factor-DNA interactions and histone modifications in wood-forming tissue. Nat. Protoc. **9:** 2180–2193.

Lin, Y.C., et al. (2014). A simple improved-throughput xylem protoplast system for studying wood formation. Nat. Protoc. **9:** 2194–2205.

Lin, Y.J., et al. (2017). Reciprocal cross-regulation of VND and SND multigene TF families for wood formation in *Populus trichocarpa.* Proc. Natl. Acad. Sci. USA **114:** E9722–E9729.

Lin, Y.C., Li, W., Sun, Y.H., Kumari, S., Wei, H., Li, Q., Tunlaya-Anukit, S., Sederoff, R.R., and Chiang, V.L. (2013). SND1 transcription factor-directed quantitative functional hierarchical genetic regulatory network in wood formation in *Populus trichocarpa.* Plant Cell **25:** 4324–4341.

Lu, S., et al. (2013). Ptr-miR397a is a negative regulator of laccase genes affecting lignin content in *Populus trichocarpa.* Proc. Natl. Acad. Sci. USA **110:** 10848–10853.

MacMillan, C.P., Mansfield, S.D., Stachurski, Z.H., Evans, R., and Southerton, S.G. (2010). Fasciclin-like arabinogalactan proteins: Specialization for stem biomechanics and cell wall architecture in Arabidopsis and Eucalyptus. Plant J. **62:** 689–703.

McCarthy, R.L., Zhong, R., and Ye, Z.H. (2009). MYB83 is a direct target of SND1 and acts redundantly with MYB46 in the regulation of secondary cell wall biosynthesis in Arabidopsis. Plant Cell Physiol. **50:** 1950–1964.

Moreno-Risueno, M.A., Busch, W., and Benfey, P.N. (2010). Omics meet networks - using systems approaches to infer regulatory networks in plants. Curr. Opin. Plant Biol. **13:** 126–131.

Müller, C.W. (2001). Transcription factors: Global and detailed views. Curr. Opin. Struct. Biol. **11:** 26–32.

Nakano, Y., Yamaguchi, M., Endo, H., Rejab, N.A., and Ohtani, M. (2015). NAC-MYB-based transcriptional regulation of secondary cell wall biosynthesis in land plants. Front. Plant Sci. **6:** 288.

Naseer, S., Lee, Y., Lapierre, C., Franke, R., Nawrath, C., and Geldner, N. (2012). Casparian strip diffusion barrier in Arabidopsis is made of a lignin polymer without suberin. Proc. Natl. Acad. Sci. USA **109:** 10101–10106.

Niu, W., et al. (2011). Diverse transcription factor binding features revealed by genome-wide ChIP-seq in *C. elegans.* Genome Res. **21:** 245–254.

Ohtani, M., Nishikubo, N., Xu, B., Yamaguchi, M., Mitsuda, N., Goué, N., Shi, F., Ohme-Takagi, M., and Demura, T. (2011). A NAC domain protein family contributing to the regulation of wood formation in poplar. Plant J. **67:** 499–512.

Osakabe, K., Tsao, C.C., Li, L., Popko, J.L., Umezawa, T., Carraway, D.T., Smeltzer, R.H., Joshi, C.P., and Chiang, V.L. (1999). Coniferyl aldehyde 5-hydroxylation and methylation direct syringyl lignin biosynthesis in angiosperms. Proc. Natl. Acad. Sci. USA **96:** 8955–8960.

Pastore, J.J., Limpuangthip, A., Yamaguchi, N., Wu, M.F., Sang, Y., Han, S.K., Malaspina, L., Chavdaroff, N., Yamaguchi, A., and Wagner, D. (2011). LATE MERISTEM IDENTITY2 acts together with LEAFY to activate APETALA1. Development **138:** 3189–3198.

Patzlaff, A., McInnis, S., Courtenay, A., Surman, C., Newman, L.J., Smith, C., Bevan, M.W., Mansfield, S., Whetten, R.W., Sederoff, R.R., and Campbell, M.M. (2003a). Characterisation of a pine MYB that regulates lignification. Plant J. **36:** 743–754.

Patzlaff, A., Newman, L.J., Dubos, C., Whetten, R.W., Smith, C., McInnis, S., Bevan, M.W., Sederoff, R.R., and Campbell, M.M. (2003b). Characterisation of Pt MYB1, an R2R3-MYB from pine xylem. Plant Mol. Biol. **53:** 597–608.

Pomar, F., Novo, M., Bernal, M.A., Merino, F., and Barcelo, A.R. (2004). Changes in stem lignins (monomer composition and crosslinking) and peroxidase are related with the maintenance of leaf photosynthetic integrity during Verticillium wilt in *Capsicum annuum.* New Phytol. **163:** 111–123.

Porth, I., Klápště, J., Skyba, O., Lai, B.S., Geraldes, A., Muchero, W., Tuskan, G.A., Douglas, C.J., El-Kassaby, Y.A., and Mansfield, S.D. (2013). *Populus trichocarpa* cell wall chemistry and ultrastructure trait variation, genetic control and genetic correlations. New Phytol. **197:** 777–790.

Ragauskas, A.J., et al. (2006). The path forward for biofuels and biomaterials. Science **311:** 484–489.

Ralph, J., MacKay, J.J., Hatfield, R.D., O'Malley, D.M., Whetten, R.W., and Sederoff, R.R. (1997). Abnormal lignin in a loblolly pine mutant. Science **277:** 235–239.

Ralph, J., Brunow, G., Harris, P.J., Dixon, R.A., Schatz, P.F., and Boerjan, W. (2008). Lignification: Are lignins biosynthesized via simple combinatorial chemistry or via proteinaceous control and template replication? Rec Adv Polyphen Res **1:** 36–66.

Ranocha, P., Chabannes, M., Chamayou, S., Danoun, S., Jauneau, A., Boudet, A.M., and Goffner, D. (2002). Laccase down-regulation

causes alterations in phenolic metabolism and cell wall structure in poplar. Plant Physiol. **129:** 145–155.

Reece-Hoyes, J.S., Diallo, A., Lajoie, B., Kent, A., Shrestha, S., Kadreppa, S., Pesyna, C., Dekker, J., Myers, C.L., and Walhout, A.J. (2011). Enhanced yeast one-hybrid assays for high-throughput gene-centered regulatory network mapping. Nat. Methods **8:** 1059–1064.

Reimand, J., Arak, T., Adler, P., Kolberg, L., Reisberg, S., Peterson, H., and Vilo, J. (2016). g:Profiler-a web server for functional interpretation of gene lists (2016 update). Nucleic Acids Res. **44:** 83-89.

Rhee, S.Y., Osborne, E., Poindexter, P.D., and Somerville, C.R. (2003). Microspore separation in the quartet 3 mutants of Arabidopsis is impaired by a defect in a developmentally regulated polygalacturonase required for pollen mother cell wall degradation. Plant Physiol. **133:** 1170–1180.

Robinson, M.D., McCarthy, D.J., and Smyth, G.K. (2010). edgeR: A bioconductor package for differential expression analysis of digital gene expression data. Bioinformatics **26:** 139–140.

Roy, S.; The modEncode Consortium, et al. (2010) Identification of functional elements and regulatory circuits by Drosophila modENCODE. Science **330:** 1787–1797.

Schmittgen, T.D., and Livak, K.J. (2008). Analyzing real-time PCR data by the comparative C(T) method. Nat. Protoc. **3:** 1101–1108.

Shi, R., Sun, Y.H., Li, Q., Heber, S., Sederoff, R., and Chiang, V.L. (2010b). Towards a systems approach for lignin biosynthesis in *Populus trichocarpa*: Transcript abundance and specificity of the monolignol biosynthetic genes. Plant Cell Physiol. **51:** 144–163.

Shi, R., Yang, C., Lu, S., Sederoff, R., and Chiang, V.L. (2010a). Specific down-regulation of PAL genes by artificial microRNAs in *Populus trichocarpa.* Planta **232:** 1281–1288.

Shi, R., Wang, J.P., Lin, Y.C., Li, Q., Sun, Y.H., Chen, H., Sederoff, R.R., and Chiang, V.L. (2017). Tissue and cell-type co-expression networks of transcription factors and wood component genes in *Populus trichocarpa.* Planta **245:** 927–938.

Solomon, M.J., Larsen, P.L., and Varshavsky, A. (1988). Mapping protein-DNA interactions *in vivo* with formaldehyde: Evidence that histone H4 is retained on a highly transcribed gene. Cell **53:** 937–947.

Song, D., Shen, J., and Li, L. (2010). Characterization of cellulose synthase complexes in Populus xylem differentiation. New Phytol. **187:** 777–790.

Song, J., Lu, S., Chen, Z.Z., Lourenco, R., and Chiang, V.L. (2006). Genetic transformation of *Populus trichocarpa* genotype Nisqually-1: A functional genomic tool for woody plants. Plant Cell Physiol. **47:** 1582–1589.

Song, L., Huang, S.C., Wise, A., Castanon, R., Nery, J.R., Chen, H., Watanabe, M., Thomas, J., Bar-Joseph, Z., and Ecker, J.R. (2016). A transcription factor hierarchy defines an environmental stress response network. Science **354:** 354.

Suzuki, S., Li, L., Sun, Y.H., and Chiang, V.L. (2006). The cellulose synthase gene superfamily and biochemical functions of xylem-specific cellulose synthase-like genes in *Populus trichocarpa.* Plant Physiol. **142:** 1233–1245.

Taylor-Teeples, M., et al. (2015). An Arabidopsis gene regulatory network for secondary cell wall synthesis. Nature **517:** 571–575.

Tian, Q., Wang, X., Li, C., Lu, W., Yang, L., Jiang, Y., and Luo, K. (2013). Functional characterization of the poplar R2R3-MYB transcription factor PtoMYB216 involved in the regulation of lignin biosynthesis during wood formation. PLoS One **8:** e76369.

Trapnell, C., Pachter, L., and Salzberg, S.L. (2009). TopHat: Discovering splice junctions with RNA-seq. Bioinformatics **25:** 1105–1111.

Vance, C.P., Kirk, T.K., and Sherwood, R.T. (1980). Lignification as a mechanism of disease resistance. Annu. Rev. Phytopathol. **18:** 259–288.

Vanholme, R., et al. (2013). Caffeoyl shikimate esterase (CSE) is an enzyme in the lignin biosynthetic pathway in Arabidopsis. Science **341:** 1103–1106.

Vermeirssen, V., Deplancke, B., Barrasa, M.I., Reece-Hoyes, J.S., Arda, H.E., Grove, C.A., Martinez, N.J., Sequerra, R., Doucette-Stamm, L., Brent, M.R., and Walhout, A.J. (2007). Matrix and Steiner-triple-system smart pooling assays for high-performance transcription regulatory network mapping. Nat. Methods **4:** 659–664.

Wang, J.P., et al. (2014a). Complete proteomic-based enzyme reaction and inhibition kinetics reveal how monolignol biosynthetic enzyme families affect metabolic flux and lignin in *Populus trichocarpa.* Plant Cell **26:** 894–914.

Wang, J.P., et al. (2018). Improving wood properties for wood utilization through multi-omics integration in lignin biosynthesis. Nat. Commun. **9:** 1579.

Wang, H.Z., and Dixon, R.A. (2012). On-off switches for secondary cell wall biosynthesis. Mol. Plant **5:** 297–303.

Wang, M.M., and Reed, R.R. (1993). Molecular cloning of the olfactory neuronal transcription factor Olf-1 by genetic selection in yeast. Nature **364:** 121–126.

Wang, J.P., Shuford, C.M., Li, Q., Song, J., Lin, Y.C., Sun, Y.H., Chen, H.C., Williams, C.M., Muddiman, D.C., Sederoff, R.R., and Chiang, V.L. (2012). Functional redundancy of the two 5-hydroxylases in monolignol biosynthesis of *Populus trichocarpa*: LC-MS/MS based protein quantification and metabolic flux analysis. Planta **236:** 795–808.

Wang, S., Li, E., Porth, I., Chen, J.G., Mansfield, S.D., and Douglas, C.J. (2014b). Regulation of secondary cell wall biosynthesis by poplar R2R3 MYB transcription factor PtrMYB152 in Arabidopsis. Sci. Rep. **4:** 5054.

Wu, A.M., Hörnblad, E., Voxeur, A., Gerber, L., Rihouey, C., Lerouge, P., and Marchant, A. (2010). Analysis of the Arabidopsis IRX9/IRX9-L and IRX14/IRX14-L pairs of glycosyltransferase genes reveals critical contributions to biosynthesis of the hemicellulose glucuronoxylan. Plant Physiol. **153:** 542–554.

Xie, M., et al. (2018). A 5-enolpyruvylshikimate 3-phosphate synthase functions as a transcriptional repressor in *Populus.* Plant Cell **30:** 1645–1660.

Yan, K.K., Fang, G., Bhardwaj, N., Alexander, R.P., and Gerstein, M. (2010). Comparing genomes to computer operating systems in terms of the topology and evolution of their regulatory control networks. Proc. Natl. Acad. Sci. USA **107:** 9186–9191.

Yang, F., et al. (2017). A maize gene regulatory network for phenolic metabolism. Mol. Plant **10:** 498–515.

Yang, Y., Park, J.W., Bebee, T.W., Warzecha, C.C., Guo, Y., Shang, X., Xing, Y., and Carstens, R.P. (2016). Determination of a comprehensive alternative splicing regulatory network and combinatorial regulation by key factors during the epithelial-to-mesenchymal transition. Mol. Cell. Biol. **36:** 1704–1719.

Ye, Z.H., Kneusel, R.E., Matern, U., and Varner, J.E. (1994). An alternative methylation pathway in lignin biosynthesis in *Zinnia.* Plant Cell **6:** 1427–1439.

Yu, H., and Gerstein, M. (2006). Genomic analysis of the hierarchical structure of regulatory networks. Proc. Natl. Acad. Sci. USA **103:** 14724–14731.

Zhong, R., and Ye, Z.H. (2012). MYB46 and MYB83 bind to the SMRE sites and directly activate a suite of transcription factors and secondary wall biosynthetic genes. Plant Cell Physiol. **53:** 368–380.

Zhong, R., Morrison III, W.H., Negrel, J., and Ye, Z.H. (1998). Dual methylation pathways in lignin biosynthesis. Plant Cell **10:** 2033–2046.

Zhong, R., Demura, T., and Ye, Z.H. (2006). SND1, a NAC domain transcription factor, is a key regulator of secondary wall synthesis in fibers of Arabidopsis. Plant Cell **18:** 3158–3170.

Zhong, R., Lee, C., and Ye, Z.H. (2010a). Functional characterization of poplar wood-associated NAC domain transcription factors. Plant Physiol. **152:** 1044–1055.

Zhong, R., Lee, C., and Ye, Z.H. (2010b). Global analysis of direct targets of secondary wall NAC master switches in Arabidopsis. Mol. Plant **3:** 1087–1103.

Zhong, R., Lee, C., McCarthy, R.L., Reeves, C.K., Jones, E.G., and Ye, Z.H. (2011). Transcriptional activation of secondary wall biosynthesis by rice and maize NAC and MYB transcription factors. Plant Cell Physiol. **52:** 1856–1871.

Zhong, R., McCarthy, R.L., Haghighat, M., and Ye, Z.H. (2013). The poplar MYB master switches bind to the SMRE site and activate the secondary wall biosynthetic program during wood formation. PLoS One **8:** e69219.

Zhu, C., Ganguly, A., Baskin, T.I., McClosky, D.D., Anderson, C.T., Foster, C., Meunier, K.A., Okamoto, R., Berg, H., and Dixit, R. (2015). The fragile Fiber1 kinesin contributes to cortical microtubule-mediated trafficking of cell wall components. Plant Physiol. **167:** 780–792.

Zhu, J., Chen, H., Li, H., Gao, J.F., Jiang, H., Wang, C., Guan, Y.F., and Yang, Z.N. (2008). Defective in Tapetal development and function 1 is essential for anther development and tapetal function for microspore maturation in Arabidopsis. Plant J. **55:** 266–277.